Issue Brief | October 2025

Monitoring Crop Residue Burning Better

Moving Beyond Fire Counts

Authors
Sneha Maria Ignatious
Rishikesh P.
Mohammad Rafiuddin

Suggested citation: Ignatious, Sneha, Rishikesh P., and Mohammad Rafiuddin. 2025. *Monitoring Crop Residue Burning Better: Moving Beyond Fire Counts*. New Delhi: Council on Energy, Environment and Water.

Disclaimer: The views expressed in this work are those of the authors and do not necessarily reflect the views and policies of the Council on Energy, Environment and Water.

Cover image: iStock. For illustrative purposes only.

Peer reviewers: Dr Tianjia Liu, Assistant Professor, University of British Columbia; Dr Prakhar Misra, Assistant Professor, Indian Institute of Technology (IIT) Roorkee; Dr C.S. Murthy, Former Director, Mahalanobis National Crop Forecast Centre, and Dr Vishwas Chitale, Fellow - CEEW.

Acknowledgments: We thank Vasudha G. and Satyam Jha, former interns at CEEW, and Navjot Singh Sarao, consultant with CEEW, for their contributions to the study.

Publication team: Purnima P. Vijaya (CEEW); Alina Sen (CEEW); Twig Designs, and FRIENDS Digital Colour Solutions.

Organisation: The **Council on Energy, Environment and Water** (CEEW)—a homegrown institution with headquarters in New Delhi—is among the **world's leading climate think tanks**. The Council is also often ranked among the **world's best-managed and independent think tanks**. It uses data, integrated analysis, and strategic outreach to explain—and change— the use, reuse, and misuse of resources. It prides itself on the independence of its high quality research and strives to **impact sustainable development at scale** in India and the Global South. In over fifteen years of operation, CEEW has impacted over 400 million lives and engaged with over 20 state governments. Follow us on LinkedIn and X (formerly Twitter) for the latest updates.

Council on Energy, Environment and Water
ISID Campus, 4 Vasant Kunj Institutional Area,
New Delhi-110070, India
T: +91 (0) 11 4073 3300
info@ceew.in | ceew.in | 𝕏 @CEEWIndia | ceewindia

Monitoring Crop Residue Burning Better

Moving Beyond Fire Counts

Issue Brief | October 2025
Sneha Maria Ignatious, Rishikesh P.,
and Mohammad Rafiuddin

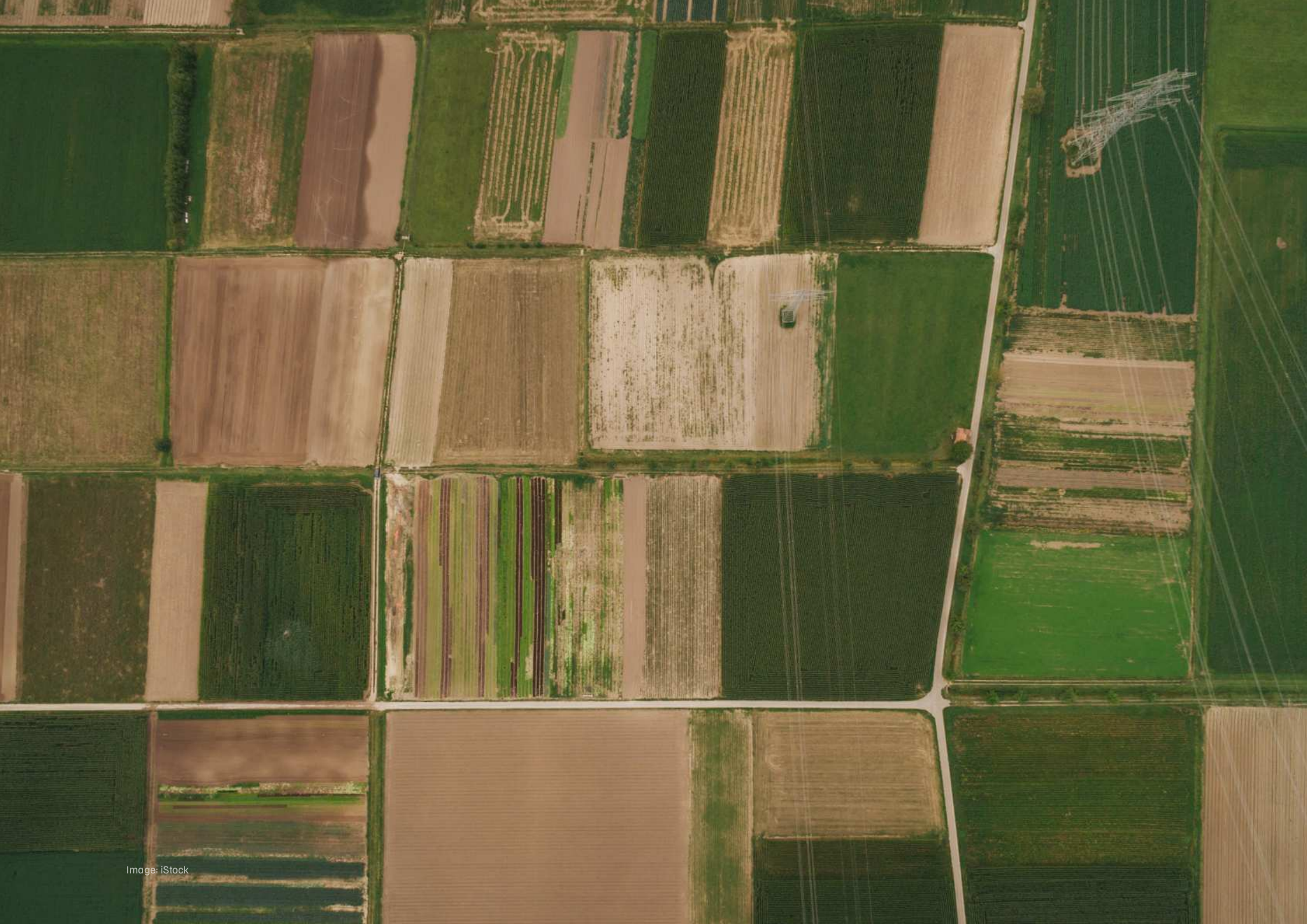

Image: iStock

About CEEW

The Council on Energy, Environment and Water (CEEW) is one of Asia's leading not-for-profit policy research institutions and among the world's top climate think tanks. The Council uses **data, integrated analysis, and strategic outreach to explain—and change—the use, reuse, and misuse of resources**. The Council addresses pressing global challenges through an integrated and internationally focused approach. It prides itself on the independence of its high-quality research, develops partnerships with public and private institutions, and engages with the wider public. CEEW is a strategic/ knowledge partner to 11 ministries for India's G20 presidency.

The Council's illustrious Board comprises Mr Jamshyd Godrej (Chairperson), Mr S. Ramadorai, Mr Montek Singh Ahluwalia, Dr Naushad Forbes, Dr Janmejaya Sinha, Dr Suresh Prabhu, and Ms Vinita Bali. The 350+ strong executive team is led by Dr Arunabha Ghosh. CEEW has repeatedly featured among the world's best managed and independent think tanks.

In over 15 years of operations, The Council has engaged in 500+ research projects, published 460+ peer-reviewed books, policy reports and papers, created 220+ databases or improved access to data, advised governments around the world 1400+ times, promoted bilateral and multilateral initiatives on 160+ occasions, and organised 610+ seminars and conferences. In July 2019, Minister Dharmendra Pradhan and Dr Fatih Birol (IEA) launched the CEEW Centre for Energy Finance. In August 2020, Powering Livelihoods—a CEEW and Villgro initiative for rural start-ups—was launched by Minister Piyush Goyal, Dr Rajiv Kumar (then NITI Aayog), and H.E. Ms Damilola Ogunbiyi (SEforAll).

The Council's major contributions include: Informing India's net-zero goals; work for the PMO on accelerated targets for renewables, power sector reforms, environmental clearances, *Swachh Bharat*; pathbreaking work for India's G20 presidency, the Paris Agreement, the HFC deal, the aviation emissions agreement, and international climate technology cooperation; the first independent evaluation of the *National Solar Mission*; India's first report on global governance, submitted to the National Security Advisor; support to the National Green Hydrogen and Green Steel Missions; the 584-page *National Water Resources Framework Study* for India's 12th Five Year Plan; irrigation reform for Bihar; the birth of the Clean Energy Access Network; the concept and strategy for the International Solar Alliance (ISA); the Common Risk Mitigation Mechanism (CRMM); India's largest multidimensional energy access survey (ACCESS); critical minerals for *Make in India*; India's climate geoengineering governance; analysing energy transition in emerging economies, including Indonesia, South Africa, Sri Lanka, and Viet Nam. CEEW published *Jobs, Growth and Sustainability: A New Social Contract for India's Recovery*, the first economic recovery report by a think tank during the COVID-19 pandemic.

The Council's current initiatives include: State-level modelling for energy and climate policies; consumer-centric smart metering transition and wholesale power market reforms; modelling carbon markets; piloting business models for solar rooftop adoption; fleet electrification and developing low-emission zones across cities; assessing green jobs potential at the state-level, circular economy of solar supply chains and wastewater; assessing carbon pricing mechanisms and India's carbon capture, usage and storage (CCUS) potential; developing a first-of-its-kind Climate Risk Atlas for India; sustainable cooling solutions; developing state-specific dairy sector roadmaps; supporting India's electric vehicle and battery ambitions; and enhancing global action for clean air via a global commission 'Our Common Air'.

The Council has a footprint in over 20 Indian states, working extensively with 15 state governments and grassroots NGOs. Some of these engagements include supporting power sector reforms in Uttar Pradesh, Rajasthan, and Haryana; energy policy in Rajasthan, Jharkhand, and Uttarakhand; driving low-carbon transitions in Bihar, Maharashtra, and Tamil Nadu; promoting sustainable livelihoods in Odisha, Bihar, and Uttar Pradesh; advancing industrial sustainability in Tamil Nadu, Uttar Pradesh, and Gujarat; evaluating community-based natural farming in Andhra Pradesh; and supporting groundwater management, e-auto adoption and examining crop residue burning in Punjab.

Image: iStock

Contents


Image: iStock

Executive summary

Crop residue burning (CRB) is a global concern with far-reaching environmental and public health implications. It releases greenhouse gases (GHGs), damages soil, causes air pollution, and places a significant burden on both the environment and human health (Ali et al. 2024). Despite these harmful effects, CRB remains a common method for clearing fields due to factors such as practicality, tradition, and perceptions regarding pest control. It is prevalent across countries such as Mexico, the United States, Brazil, China, and India (World Bank n.d.).

India generates around 754 million tonnes of crop residue annually, of which 228 million tonnes are surplus (MNRE n.d.). Punjab alone produces about 20 million tonnes of crop residue annually from paddy cultivation (PIB 2023b). Paddy is the leading kharif crop in Punjab, sown on around 30 lakh hectares, accounting for nearly 60 per cent of the state's area. Farmers manage the straw generated after paddy harvest in three ways: in-situ management, ex-situ management, and burning. In-situ methods involve incorporating the straw back into the soil using machines such as the Happy Seeder and Super Seeder (Erbaugh et al. 2024). Ex-situ methods manage straw outside the fields, converting it into value-added products (ICAR 2021).

However, due to the challenges associated with these methods—such as financial constraints, limited availability of machinery, and misconceptions about the productivity impacts of residue management methods—a large share of farmers continue to practice burning. It offers the cheapest and quickest way of clearing stubble within the short window between harvest and rabi crop sowing (Erbaugh et al. 2024). This practice remains a significant contributor to air pollution in the Indo-Gangetic Plain (IGP) region, particularly during the months of October and November (Jethva et al. 2019; Lin and Begho 2022). For example, CRB contributes up to 35 per cent of PM2.5 in Delhi during the peak burning period (Govardhan et al. 2023).

Crop Residue Management methods encompass both in-situ and ex-situ methods.

Farmers burn stubble in two ways—completely or partially (Gupta 2010). In complete burning, the entire leftover straw is set on fire, whereas in partial burning, only the loose straw left after running the harvester is burnt (Kumar et al. 2015; Gupta 2010; Kemanth et al. 2024). A 2022 study found that about 58 per cent of Punjab's farmers practised in-situ methods, but more than half of them also practised partial burning before using machines to clear their fields (Kemanth et al. 2024).

To curb CRB, the Punjab state government banned the practice in 2013 (NGT 2023). The National Green Tribunal (NGT) also prohibited it in 2015 (PIB 2019). The Union government has also introduced various schemes and issued directives to promote the use of crop residue management (CRM) machines and ex-situ management.

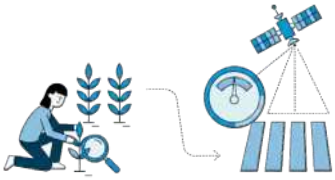

Crop residue monitoring uses both ground observations and satellite data, with satellites offering a faster, more practical approach

Crop residue burning tracking uses satellite data or on-ground observations, with satellites offering a faster and more practical option. Satellite-borne instruments such as the Visible Infrared Imaging Radiometer Suite (VIIRS) and the Moderate Resolution Imaging Spectroradiometer (MODIS) detect active fire incidents. Burnt area measurement using satellite imagery from Sentinel-2, Landsat, and other sources, or derived from MODIS and VIIRS observations, is another monitoring method. Deploying personnel on the ground and recording CRB incidents manually is labour-intensive.

Remote sensing–based methods have limitations like coarse spatial and temporal resolution, inability to see through fog, smoke, clouds, etc. Moreover, farm characteristics can change rapidly, and if the satellites pass after they change, the sensors may fail to record burning. More importantly, fire count and burnt-area methods capture the extent of CRB to a limited degree–they do not reveal whether the detected fields are burnt partially or completely.

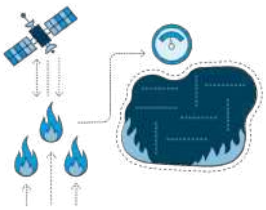

Fire counts indicate the number of fire incidents, and the burnt area represents the field area burnt

In India, the Indian Space Research Organisation (ISRO) monitors CRB. It uses fire-count data from the VIIRS onboard the Suomi National Polar-Orbiting Partnership (SUOMI NPP) and the MODIS onboard the Aqua and Terra satellites (CAQM 2021a). The National Remote Sensing Centre (NRSC) of the ISRO computes burnt area using the Mid-Infrared Burn Index (MIRBI) and publishes bulletins (NRSC-ISRO 2022). However, these burnt area data are not publicly available.

According to official fire-count data, Punjab recorded around 10,000 active fire incidents in the 2024 kharif season (CREAMS n.d.). This is the lowest since 2018, when fire counts in the state exceeded 55,000 (Kurinji and Prakash 2021). However, experts dispute these figures, arguing that farmers burn stubble after the satellite has passed overhead (NASA 2025; Misra et al. 2025). Taking cognisance of these concerns, the Supreme Court (SC) instructed the Union government and the Commission for Air Quality Management in National Capital Region and Adjoining Areas (CAQM) to obtain data from additional satellites such as the Geostationary Korea Multi-Purpose Satellite-2A (GEO-KOMPSAT-2A). Additionally, the CAQM ordered intensified patrolling during the late evening hours to monitor incidents of bypassing satellites (CAQM 2025).

This results in an inaccurate estimation of the extent of CRB. This, in turn, leads to lower emission estimates and inaccuracies in air-quality models that rely on these emission estimates for inputs. Uncertainties in both fire counts and burnt-area estimates also lead to uncertainties in understanding the effectiveness of CRB mitigation policies.

In this study, we evaluate the following questions:

- To what extent do satellite-derived fire counts represent the actual extent of crop residue burning?
- Can burnt area indices (indicators applied to satellite imagery to compute how much land has burned) reliably detect burnt fields, and can they differentiate between completely and partially burnt fields?

Data and methodology

We used very-high-resolution satellite imagery from the archived images available on Google Earth Pro from Maxar as the ground truth data. Of all the archived images available on Google Earth Pro between 2019 and 2025, we could only identify a region in Sangrur district, where the images were available for two consecutive days. We counted the number of fields burnt from the images and compared it with those detected by VIIRS and MODIS.

We used an algorithm that combines two indices, the Burnt Area Index for Sentinel-2 (BAIS2) and the Tasseled Cap Brightness Index (TBI), to compute burnt area from openly available Sentinel-2 imagery. We used the very-high-resolution imagery from Maxar across multiple regions in Punjab as the ground truth data to compute the accuracy of our burnt area algorithm. We propose first-of-their-kind methods to differentiate between partially and completely burnt fields. They rely on the hypotheses that either a threshold exists to differentiate between the two types of fields reliably or the number of pixels detected in a partially burnt field is lower than that in a completely burnt field.

Satellite-borne sensors such as the VIIRS and the MODIS capture fewer farm fire incidents than actually occur

Results

- **Satellite sensors are unable to fully capture the extent of fire incidents**: Analysis of very high-resolution images from two consecutive days in November 2020 showed that 169 fields were either completely or partially burnt. In comparison, VIIRS detected only seven fires, and MODIS detected none, suggesting that satellite-borne sensors may not fully detect all fire events in the region. However, this is an estimate based on one instance in 2020 due to limited data availability.

- **Combining BAIS2 and TBI detects burnt area with 75 per cent accuracy**: The study tested the effectiveness of two indices—BAIS2 (Burned Area Index for Sentinel-2), a char sensitive index which identifies burnt areas based on changes in surface reflectance, and TBI (Tasseled Cap Brightness Index), which relies on the degree of the brightness of a surface to identify burnt areas. When used together, these indices provided a more reliable classification of burnt and unburnt fields than either index alone. The combined threshold achieved a detection accuracy of 75 per cent with minimal false positives.

- **Differentiating between partially and completely burnt fields is more difficult than detecting burnt fields**: While the algorithm designed to detect a burnt field detected burnt fields with an accuracy of 75 per cent, the proposed method, optimised for detecting only completely burnt fields, achieved only 39 per cent accuracy when applied to both types. An alternate approach—classifying fields by the number of burnt pixels—was also unsuccessful, underscoring the complexity of detecting heterogeneous burn patterns.

Limitations

While the algorithm performs well in accurately detecting burnt fields and pixels, our study has certain limitations. Missing data due to the five-day revisit time of Sentinel-2, loss of data due to clouds and smoke, the exclusion of fields managed through in-situ methods under unburnt fields, misclassification of irrigated fields as burnt fields, and the inability to differentiate between partially and completely burnt fields, even at a very high resolution, are the limitations of this study.

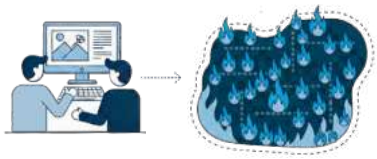

Central and state government agencies should use very-high-resolution satellite imagery to monitor crop residue burning incidents, along with fire counts and burnt area

Conclusion and recommendations

Our analysis of very-high-resolution satellite imagery from two consecutive days, obtained for a selected region of 74 sq km, shows that the satellite-borne fire-counting sensors detect only a portion of the fires observed in the imagery. We identified 169 burnt fields over the selected region over two days. However, the sensors could detect only seven fire incidents on these days.

Our analysis of an alternative method for monitoring CRB, including the computation of burnt area, shows that the burnt area indices BAIS2 and TBI can differentiate between burnt and unburnt fields. We observed that a combination of BAIS2 and TBI performs well with the fewest false positives. It could detect the burnt pixels with an accuracy of 75 per cent. After testing two methods to separate partially and completely burnt fields, we conclude that it is challenging to differentiate between them. Based on our learnings from the study, we recommend the following:

- **Central and state government agencies should use very-high-resolution satellite imagery to monitor CRB incidents, along with fire counts and burnt area**. While the cost associated with satellite imagery limits extensive usage, agencies should consider using very-high-resolution images from commercial satellite imagery providers, such as Maxar Technologies and Planet Labs, at least during a portion of the burning season.

- **The Indian Institute of Tropical Meteorology (IITM) and the India Meteorological Department (IMD) should use burnt area estimates along with fire counts to accurately estimate the emissions from CRB**. Using these estimates may improve the performance of the Air Quality Early Warning System (AQEWS), which provides air quality forecasts for Delhi and other cities.

- **India's future space programmes should include at least two satellites to complement the Sentinel-2 constellation**. India's own satellite constellation will enable the collection of data at a high temporal resolution, compared to the current five-day revisit time of Sentinel-2.

1. Introduction

Crop residue burning (CRB) is a global concern with far-reaching environmental and health impacts. It exacerbates soil erosion (Lin and Begho 2022) and reduces soil fertility by removing essential nutrients and microorganisms. It also impairs crop health (Abdurrahman et al. 2020). CRB releases harmful pollutants, such as carbon dioxide (CO2), carbon monoxide (CO), and particulate matter (PM), into the atmosphere (Pinakana et al. 2024), which impact public health adversely (TERI 2021).

Globally, farmers burn an estimated 450 million tonnes of crop residue each year (CCAC 2023). The United States ranks third in greenhouse gas (GHG) emissions from crop residues (Pinakana et al. 2024). Brazil burns about 3.2 million tonnes of rice straw annually (G. Singh et al. 2021). In Indonesia, approximately 45 million tonnes of crop residue are burnt annually (Andini et al. 2018), whereas 100 million tonnes are burnt in China (Li et al. 2022).

According to the Sardar Swaran Singh National Institute of Bio-Energy, India generates around 754 million tonnes of crop residue annually—of which 228 million tonnes is surplus (MNRE n.d.)—mainly from crops such as rice, wheat, and sugarcane. India is the second-largest rice-producing country in the world (USDA 2025), and Punjab is the fourth-largest rice-producing state in the country (UPAg, DoAFW n.d.). Farmers in Punjab predominantly follow a two-crop cycle, growing wheat during the rabi season (November–April) and paddy during the kharif season (May–October) (Kingra et al. 2017). Paddy cultivation spans approximately 31 lakh hectares (3.1 million hectares) in Punjab, yielding around 20 million tonnes of paddy straw annually (NGT 2024).

Crop residue management (CRM) methods encompass both in-situ and ex-situ approaches. In in-situ management, the stubble is incorporated back into the soil using machines such as the Super Seeder and Happy Seeder (Dhaliwal n.d.; Singh et al. 2024). In ex-situ management, the stubble gets transported off the farm and finds use in facilities such as compressed biogas (CBG) plants and thermal power plants to generate value-added products, including biogas and electricity (ICAR 2021). However, a significant proportion of farmers continue to burn straw in the field (PIB 2024). Misconceptions associated with reduced productivity from CRM machines, fears of pest attacks, the short 20–25 day window between the harvest and sowing of the rabi crop, and the higher operating costs of CRM machinery contribute to this practice (ICAR 2021; Kemanth et al. 2024). This practice of burning is a leading contributor to the increased levels of air pollution in the Indo-Gangetic Plain (IGP) region during the winter months. For instance, CRB contributes up to 30–35 per cent of Delhi's PM2.5 during peak burning period (Govardhan et al. 2023).

Inaccurate estimates of crop residue burning distort emission calculations, compromising the performance of air quality models

To curb CRB, the central and state governments have introduced a range of schemes and measures. A brief chronology of the measures is as follows:

- **2013**: The state government of Punjab banned CRB (NGT 2023).
- **2014**: The Ministry of Agriculture and Family Welfare (MoAFW) launched the *Sub-Mission on Agricultural Mechanization* (SMAM) to extend agricultural mechanisation to small and marginal farmers and promote custom hiring centres (CHCs) (MoAFW 2018).
- **2015**: The National Green Tribunal (NGT) also banned CRB (NGT 2023).
- **2018**: The union government launched the *Central Sector Scheme for Promotion of Agricultural Mechanization for In-Situ Management of Crop Residue*. The scheme provides a 50 per cent subsidy to individual farmers and an 80 per cent subsidy to registered farmer groups, cooperative societies, and farmer producer organisations (FPOs) for the procurement of CRM machines (PIB 2021).
- **2018**: The Ministry of Petroleum and Natural Gas (MoPNG) launched the *Sustainable Alternative Towards Affordable Transportation* (SATAT) scheme to encourage entrepreneurs to set up CBG plants and establish an enabling ecosystem (MoPNG n.d.).
- **2018**: The MoPNG also launched the *National Policy on Biofuels* to increase the use of biofuels in the energy and transportation sectors, aiming to enable the availability of biofuels in the market to increase the blending percentage (MoPNG 2018).
- **2022**: The Commission for Air Quality Management in National Capital Region and Adjoining Areas (CAQM) mandated all thermal power plants (TPPs) within a 300-kilometre radius of Delhi to co-fire 5–10 per cent biomass alongside coal (CAQM 2022).
- **2024**: The MoPNG launched the *Biomass Aggregation Scheme* to support biomass collection for biomass-based CBG plants by providing financial assistance to CBG producers for the procurement of biomass aggregation machinery (MoPNG 2024).

Despite these efforts, Punjab recorded around 10,000 active fire incidents in 2024 (ICAR 2024). The actual number may be significantly higher, as many farmers may have started to burn stubble after the satellites pass (NASA 2025; Misra et al. 2025). Recent studies claim an increase in the adoption of in-situ machinery to manage fields, with approximately 58 per cent of farmers in Punjab adopting it in 2022. However, nearly half of them also practised partial burning before using the CRM machines (Kemanth et al. 2024). In the case of partial burning, only the loose straw left behind on the field after running the harvester is burnt; however, in the case of complete burning, all post-harvest straw is set on fire (Kumar et al. 2015; Gupta 2010; Kemanth et al. 2024).

a. Completely burnt field

b. Partially burnt field

Images: CEEW

In complete burning, farmers burn all the straw remaining after harvest, whereas in partial burning, only the loose straw left after using a harvester is burnt

Authorities deploy field officers and utilise two remote sensing–based metrics–active fire counts and burnt area–to monitor CRB incidents (Hindustan Times 2023). Deploying personnel on the ground and manually recording burnt fields is labour-intensive. Therefore, remote sensing methods are highly feasible. The two metrics are as follows:

- **Fire counts**: Sensors such as the Visible Infrared Imaging Radiometer Suite (VIIRS) and the Moderate Resolution Imaging Spectroradiometer (MODIS) onboard satellites detect active fire incidents (NASA n.d.a). These sensors rely on thermal anomalies to detect fire incidents (GWIS, n.d.).

- **Burnt area**: There are two ways of burnt area estimation. The first method utilises fire-count data while the second employs burnt area indices applied to spectral measurements from satellite-borne instruments. The first method considers a fixed area surrounding the location of the detected fire as the burnt area (Ambulkar et al. 2025). The second method presupposes that the spectral signature of a field differs before and after burning. Researchers have designed various burnt area indices, such as the Tasseled Cap Brightness Index (TBI), Burnt Area Index for Sentinel-2 (BAIS2), Normalised Burn Ratio (NBR), Normalised Burn Ratio 2 (NBR2), Burn Area Index (BAI), and Mid-Infrared Burn Index (MIRBI), based on this principle (Kouadio et al. 2023).

Several researchers have attempted to compute the extent of CRB and the related challenges in India and abroad using satellite imagery, fire-count data, and ground surveys (Li et al. 2022; Mohammad et al. 2023; Singh et al. 2021; Kumar et al. 2025; Sehgal et al. 2021; Liu et al. 2019). In India, the Indian Space Research Organisation (ISRO) records and monitors fire incidents and burnt areas. It relies on VIIRS data from the Suomi National Polar-Orbiting Partnership (SUOMI NPP) satellite and MODIS data from the Aqua and Terra satellites to track active fire incidents (CAQM 2021a).

According to the burnt area estimates released by the National Remote Sensing Centre (NRSC), ISRO, Hyderabad, burnt area computation uses the burnt area index MIRBI using Sentinel-2 data (NRSC-ISRO 2022). However, Deshpande et al. (2022) have found that MIRBI's ability to separate burnt and unburnt pixels is lower compared with that of indices such as BAIS2 and TBI. Moreover, the NRSC has not made the detailed methodology or state-level burnt area estimates publicly available.

Several uncertainties are associated with remote-sensing methods:

- **Coarse spatial resolution**: Sensors only detect fires that are active during the satellite overpass time. The SUOMI NPP/VIIRS[1] passes over the IGP region around 01:30 a.m. and 01:30 p.m. local time, while the Aqua and Terra[2] satellites pass over India just after 10:30 a.m. and 01:30 p.m. (Payra et al. 2023). The revisit times of VIIRS and MODIS are 12 hours (Schroeder et al. 2014; Parkinson 2022). Satellites fail to detect fires occurring before or after the overpass times, resulting in an underestimation of fire incidents (Fusco et al. 2019). The spatial resolution of VIIRS is 375 m and that of MODIS is 1 km (NASA Earthdata 2024). Therefore, fires over areas smaller than 375 m or 1,000 m may fail to get detected by these instruments. For instance, the average size of farmland in Punjab is 4 hectares (40,000 sq m), which is smaller than the 375 m x 375 m resolution offered by VIIRS (Kurinji and Prakash 2021). In addition, small, localised fires may not result in strong enough thermal anomalies for the instruments to capture them (Jaffe et al. 2020; Zhang et al. 2021; Chen et al. 2022). Additionally, partial burning lasts only a few hours, making it difficult for satellites to detect (Kemanth et al. 2024). Studies have attempted to complement satellite data with household surveys and crop statistics to reduce uncertainties; however, this remains a significant challenge in satellite-based monitoring of CRB (Liu et al. 2020).

- **Coarse temporal resolution**: Sentinel-2 multispectral instruments offer a spatial resolution of 10–60 m but have a revisit time of five days (ESA n.d.). Harmonised Landsat and Sentinel-2 (HLS) images are available with a temporal resolution of 2–3 days, while the spatial resolution is 30 m (NASA n.d.).

- **Obstructions**: Clouds, smoke, and smog obscure active fire and burnt area detection using remote-sensing methods (Copernicus n.d.; Luft et al. 2022).

- **Surface reflectance variability**: The spectral characteristics of burnt fields can vary with time (Singh et al. 2021), and longer satellite revisit times pose a challenge, as the burnt area indices may fail to detect such farms due to a change in characteristics.

- **Incomplete information**: Both the fire count and burnt area methods cannot differentiate between partially burnt fields and completely burnt fields. Moreover, no study has attempted to distinguish between partially and completely burnt fields yet. A clear distinction between partially burnt fields and completely burnt fields is crucial for accurately estimating emissions and assessing the extent of CRM adoption.

1. VIIRS is onboard NOAA-20 and NOAA-21 satellites along with SUOMI NPP (NASA n.d.a).
2. Aqua and Terra satellites will begin shutting down in 2026/2027.

These limitations result in an underestimation or overestimation of CRB. This, in turn, has significant consequences:

- **Underestimation of emissions from CRB**: Emission inventories (EIs)—such as the Fire INventory (FINN) from the National Centre for Atmospheric Research (NCAR)—rely on fire counts to estimate CRB emissions (Wiedinmyer et al. 2023). Chemical transport models (CTMs), widely used to model air pollution, use these EIs as inputs to account for such emissions. For instance, India's CTM-based Air Quality Early Warning System (AQEWS) incorporates the FINN EI to account for CRB emissions (Govardhan et al. 2024). Uncertainties also arise from differences in fuel-loading ratios and emission factors across global EIs (Hua et al. 2024). The CAQM implements the *Graded Response Action Plan* (GRAP) in Delhi based on AQEWS forecasts (PIB 2023a). Reliable and accurate EIs are therefore essential for accurate forecasting.

- **Difficulty in assessing the impact of mitigation policies**: Both the union and state governments allocate significant financial resources to the policies aimed at curbing CRB. For instance, the union government spent approximately INR 3,600 crore under the *Central Sector Scheme for Promotion of Agricultural Mechanization for In-Situ Management of Crop Residue* between 2018 and 2024 (PIB 2025). Government sources use fire-count data to measure the success of such schemes. However, a change in fire counts should not be the sole metric to gauge the effectiveness of these policies. The Supreme Court recently noted the CAQM's observation that farmers were bypassing satellite monitoring and that the burnt area was increasing over the years, despite a decrease in fire counts. Following this, it directed the CAQM to submit fire-count data from geostationary satellites such as the Geostationary Korea Multi-Purpose Satellite-2A (GEO-KOMPSAT-2A), not just from polar-orbiting satellites (SCO 2024). Moreover, the CAQM also directed enforcement agencies to increase patrolling during the evening hours to monitor such bypassing incidents (CAQM 2025). News reports also suggest that some farmers have shifted to partial burning, resulting in a reduction in emissions from CRB (Newslaundry 2022). However, there are no scientific studies quantifying these changes.

The CAQM monitors CRB incidents using a protocol developed by ISRO (CAQM 2021b). However, as discussed earlier, farmers may have started to burn after satellite overpasses to avoid detection. Therefore, it is crucial to understand the extent to which satellite-borne sensors detect active fires and whether burnt area can complement or substitute for fire counts in monitoring CRB. It is also equally important to determine whether burnt area–based methods can capture partially burnt fields and differentiate them from completely burnt fields.

Through this study, we aim to:

- Assess the extent to which the fire count–based methods capture actual burning.
- Develop a methodology to compute burnt area.
- Test whether burnt area methods can differentiate partially burnt fields from completely burnt fields.

Our analysis focuses on Punjab during the post-kharif harvest period, when farmers typically burn paddy residue.

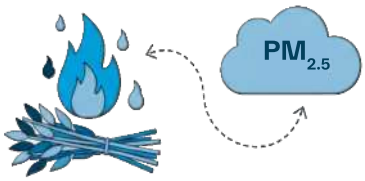

Accurate crop residue burning estimates will help evaluate the effectiveness of CRB mitigation policies

Image: iStock

2. Data and methodology

We used openly available VIIRS data and very-high-resolution satellite imagery to assess the extent to which CRB incidents get captured by satellite-borne sensors. Alongside, we also used Sentinel-2 multispectral imagery to develop an algorithm based on spectral indices to estimate the burnt area.

2.1 Data

We obtained fire-count data from the VIIRS instrument onboard the SUOMI NPP satellite and the MODIS instrument onboard the Aqua and Terra satellites. To identify burnt and unburnt fields for training and validating the algorithm, we relied on openly available very-high-resolution archived imagery from Maxar Technologies available on Google Earth Pro. We applied our algorithm to band data from the multispectral sensor onboard the Sentinel-2 satellites (NASA n.d.b).

2.2 Methodology

Assessing the ability of satellite-borne sensors to capture crop residue burning incidents

We identified a region of approximately 74 sq km in Sangrur where Google Earth Pro images were available for two consecutive days—9 and 10 November 2020. Images from the two successive days helped us identify the fields that were initially unburnt but were burnt on either of the two days. If a field that appeared unburnt appears black on the second day's image, it implies that the field was set on fire during the interval between the image acquisition times. Among archived images available on Google Earth Pro between 2019 and 2025, we could only identify this region in Sangrur with such consecutive-day coverage.

We then visually identified the fields that were unburnt on the first day and burnt on the second day. We considered a field burnt if it appeared black or grey in the image on the second day but not on the first. An unburnt field appears golden-yellow or green in the images. Figure 1 illustrates fields from both dates over a subset of the study region, along with the fields we identify as burnt. We also obtained the locations and fire counts detected by the VIIRS instrument (at all confidence levels) over the selected region. The MODIS instruments did not capture any active fire incidents over this region on these two days. We then compared the number and locations of burnt fields identified through imagery with the active fires detected by VIIRS.

Figure 1. Very-high-resolution satellite imagery obtained for two consecutive days help identify fields burnt on each day

a. Very-high-resolution satellite image captured on 9 November 2020

b. Very-high-resolution satellite image captured on 10 November 2020

Source: Google Earth Pro

Note: The marked fields are those fields which appeared unburnt on 9th and burnt on 10 November.

Assessing the performance of the burnt area indices in detecting burnt and unburnt pixels

Algorithm

Our algorithm involved applying burnt area indices to Sentinel-2 imagery to distinguish between burnt and unburnt fields. We focused on two indices—BAIS2 and TBI—and applied them to the Sentinel-2 band data to assess their ability to detect burnt fields and differentiate between completely and partially burnt fields. While BAIS2 is an ash and charcoal sensitive index which uses spectral characteristics of the red edge and short wave infrared bands of Sentinel-2, TBI is a brightness index which measures the brightness of a surface. Deshpande et al. assessed the separability index to evaluate how well different burnt area indices differentiated burnt and unburnt pixels. The study found that the separability index of BAIS2 and TBI is higher than that of indices such as MIRBI, Normalised Burn Ratio (NBR), etc (Deshpande et al 2022).

We obtained very-high-resolution satellite imagery from Google Earth Pro for dates where Sentinel-2 data are also available. We could only identify four such dates between 2019 and 2025 in Punjab during the peak burning season (between 15 October and 30 November). For the training dataset, we identified a ~220-sq km region in Sangrur where very-high-resolution imagery from Google Earth Pro and Sentinel-2 multispectral satellite imagery were available on the same date (10 November 2020). Using this imagery, we visually classified fields as partially burnt, completely burnt, and unburnt. A completely burnt field appears entirely black in the images. However, a partially burnt field appears black, interspersed with regularly spaced golden-yellow patches along its length, corresponding to the unburnt residue that is later incorporated into the soil using CRM machines. We mark two types of fields as unburnt: the ones that appear golden-yellow and those that appear green. We excluded in-situ managed fields from the unburnt category, as these were challenging to identify reliably from satellite imagery. Figure 2 illustrates the different field types.

Figure 2. In very-high-resolution satellite imagery, a completely burnt field appears entirely black, while a partially burnt field shows black areas interspersed with regularly spaced golden-yellow patches

a. Completely burnt field

b. Partially burnt field

c. Unburnt golden-yellow field

d. Unburnt green field

Source: Google Earth Pro

Note: The marked areas represent sample fields classified as completely burnt, partially burnt, unburnt (golden-yellow), and unburnt (green).

We then mapped these fields onto Sentinel-2 imagery using Google Earth Engine (GEE). We extracted the pixels from within these fields by drawing polygons within corresponding field boundaries using the Polygon drawing tool (or 'Draw a shape') available on GEE. We avoided the pixels along the edge of the field boundaries to prevent the inclusion of pixels from neighbouring fields. Figure 3 illustrates the sample polygons that we drew on GEE to extract the pixels. We then applied BAIS2 and TBI to the Sentinel-2 band data for these pixels. Annexure 1 explains the formula behind these indices and the spectral bands used to compute them.

Figure 3. Burnt area indices were computed from Sentinel-2 pixels for fields mapped using very-high-resolution imagery

Figure 3A. Different types of fields identified using Google Earth Pro

Figure 3B. Images obtained from Sentinel-2 for corresponding fields identified using Google Earth Pro

Completely burnt field

Partially burnt field

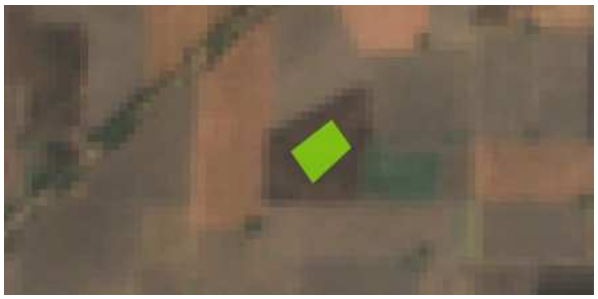

Unburnt field

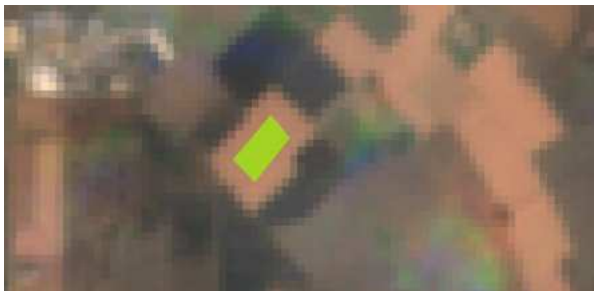

Source: Google Earth Pro and authors' analysis of Sentinel-2 data from Google Earth Engine
Note: The images shows fields identified using very-high-resolution satellite imagery from Google Earth Pro and corresponding images mapped using Sentinel-2 imagery.

Thereafter, we analysed the histograms of BAIS2 and TBI for pixels from unburnt, partially burnt, and completely burnt fields to identify the thresholds that could potentially separate these categories. We tested the performance of BAIS2 and TBI separately as well as together. For this, we analysed the histograms of burnt and unburnt field pixels as discussed in Deshpande et al. (2022) and set the thresholds based on percentiles. Deshpande et al. (2022) set the 5^{th} and 95^{th} percentiles of the indices as the lower and upper thresholds to avoid overlapping pixels and outliers. However, we did not cap the index values at both ends. The theoretical minimum value of TBI is zero (Annexure 1), corresponding to a perfectly black field. The BAIS2 value of burnt scar ranges between −1 and 1, and it is between 1 and 6 for active fires (Alcaras et al. 2022). Therefore, a cap on the BAIS2 values might cause the algorithm to miss fields that are actively burning. Hence, we did not cap the maximum value of BAIS2 or the minimum value of TBI.

Setting the thresholds

Our analysis of the BAIS2 and TBI values for different types of fields in the training dataset shows that both indices can potentially distinguish between unburnt and burnt fields. Figure 4 shows the histograms of BAIS2 and TBI of completely burnt, partially burnt, and unburnt pixels.

Figure 4. Tasseled Cap Brightness Index (TBI) and Burnt Area Index for Sentinel-2 (BAIS2) can potentially separate unburnt, partially burnt, and completely burnt fields

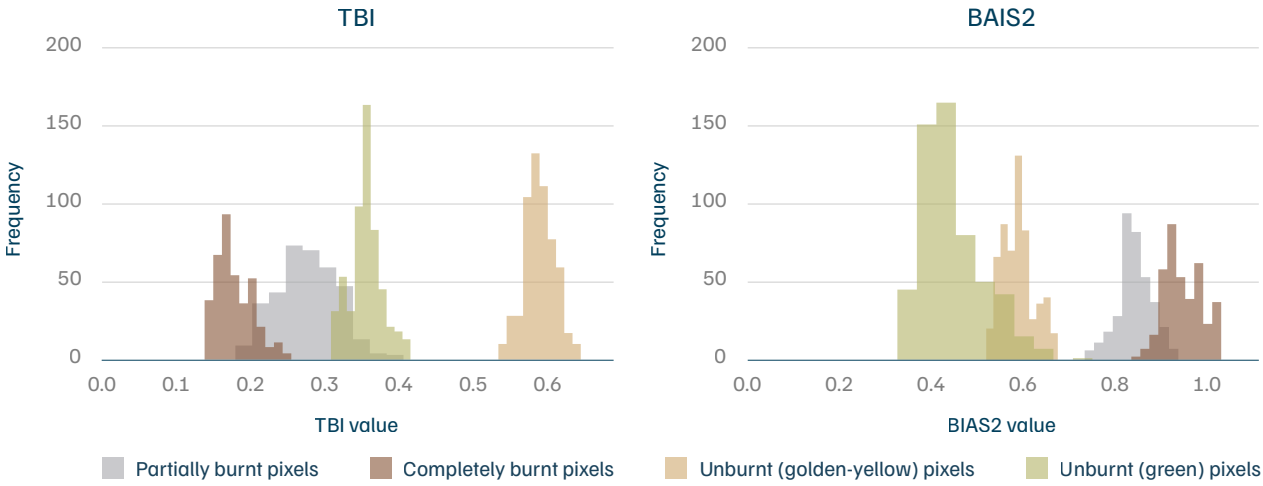

Source: Authors' analysis

However, as Figure 4 shows, TBI values for green and burnt fields overlap, while BAIS2 values for golden-yellow and burnt fields lie close together. To test whether combining thresholds improves classification, we analysed BAIS2 and TBI jointly rather than individually. Deshpande et al. (2022) also used a combined approach, capping the values of these indices between the 5th and 95th percentiles. In our case, we selected the threshold values – T1, T2, and T3 based on the index values obtained for partially burnt fields, ensuring that our algorithm captured both partially and completely burnt fields. Table 1 lists the thresholds used.

Table 1. Thresholds tested in this study to distinguish between burnt and unburnt fields

Threshold	Description
Threshold 1 (T1)	BAIS2 >= 5th percentile value of partially burnt pixels
Threshold 2 (T2)	TBI <= 95th percentile value of partially burnt pixels
Threshold 3 (T3)	BAIS2 >= 5th percentile value of partially burnt pixels TBI <= 95th percentile value of partially burnt pixels

Source: Authors' analysis

From the training dataset, we identified the values of these thresholds. We have summarised the values in Table 2.

Table 2. Values of the thresholds identified from the training dataset

Threshold	Threshold value
Threshold 1 (T1)	BAIS2 >= 0.78
Threshold 2 (T2)	TBI <= 0.34
Threshold 3 (T3)	BAIS2 >= 0.78 TBI <= 0.34

Source: Authors' analysis

Validation

To validate the algorithm's performance, we identified a test region in Punjab where the image dates of the very-high-resolution imagery from Google Earth Pro coincided with Sentinel-2 multispectral imagery. Suitable images were available for 29 October 2021, covering Hoshiarpur and Jalandhar. We then applied threshold T3 to 10 randomly selected villages across this region, which spans an area of approximately 28 sq km. Within these fields, we marked burnt fields and their field boundaries, extracted the pixels from within the fields, and created subsets of partially burnt, completely burnt, and unburnt fields. In total, we identified 287 burnt fields and 95 unburnt fields across the 10 villages. Of the 287 burnt fields, we could only clearly identify 72 completely burnt fields and 190 partially burnt fields.

We analysed the performance of the algorithm using two criteria:

- **Ability to detect burnt fields accurately**: The effectiveness of our algorithm depends on how accurately it detects both partially and completely burnt fields while avoiding unburnt fields. The algorithm is said to detect a field if it detects at least one pixel within the field. This corresponds to an area of 100 sq m.

- **Ability to detect burnt pixels accurately**: Accurate computation of burnt area requires accurate detection of all burnt pixels while minimising the detection of the unburnt ones. Using the matrix in Table 3, we computed accuracy, true positive rate (TPR), false positive rate (FPR), false negative rate (FNR), F1 score, Matthews correlation coefficient (MCC), and Cohen's kappa (k). Table 4 presents the metrics and formulas used.

Table 3. The confusion matrix used for computing performance metrics

		Observed	
		Number of burnt pixels	**Number of unburnt pixels**
Detected	**Number of burnt pixels**	True positive (TP)	False positive (FP)
	Number of unburnt pixels	False negative (FN)	True negative (TN)

where,
True positives are the burnt pixels correctly detected as burnt by the algorithm.
False negatives are the burnt pixels incorrectly classified as unburnt.
False positives are the unburnt pixels incorrectly classified as burnt.
True negatives are the unburnt pixels correctly classified as unburnt.

Source: Authors' compilation

Table 4. List of performance metrics used in the study

Metric	Description	Formula	Range of values
Accuracy	The model's ability to correctly detect burnt and unburnt pixels.	$(TP + TN)/(TP + FP + FN + TN)$	0–1 Higher is better
True positive rate (TPR)	The algorithm's ability to correctly classify a burnt pixel as burnt.	$TP/(TP + FN)$	0–1 Higher is better
False positive rate (FPR)	The algorithm's tendency to detect an unburnt pixel as burnt.	$FP/(FP + TN)$	0–1 Lower is better
False negative rate (FNR)	The algorithm's tendency to classify a burnt pixel as unburnt.	$FN/(TP + FN)$	0–1 Lower is better
F1 score	How well the algorithm identifies a burnt pixel.	$2TP/(2TP + FP + FN)$	0–1 Higher is better
Matthews correlation coefficient (MCC)	The algorithm's ability to correctly classify burnt and unburnt pixels.	$\frac{(TP \times TN - FP \times FN)}{\sqrt{(TP+FN) \times (TP+FP) \times (TN+FP) \times (TN+FN)}}$	−1–1 1 represents perfect prediction
Cohen's kappa (k)	Similar to MCC; uses all four metrics – TP, FP, FN, TN.	$(Po-Pe)/(1-Pe)$, $Po = (TP+TN)/(TP+TN+FN+FP)$ $Pe = \frac{(((TP+FN) \times (TP+FP)) + ((FN+TN) \times (FP+TN)))}{(TP+TP+FN+FP)^2}$	−1–1 Higher is better

Source: Authors' compilation

Assessing the ability of the algorithm to differentiate between partially and completely burnt fields

To assess the algorithm's ability to differentiate between partially and completely burnt fields, we computed the percentage of pixels detected in each field type. We hypothesised that the number of pixels detected by the algorithm in a partially burnt field should be lower than in a completely burnt field. We tested this hypothesis using two approaches: one threshold combination designed to detect both partially and completely burnt fields and another designed to detect only completely burnt fields.

- **Method 1**: We applied the threshold combination that detects both partially and completely burnt fields. We then computed the percentage of pixels detected as burnt in the fields and analysed if the percentage of pixels detected is different in the two types of fields and if it can potentially separate them.

- **Method 2**: We defined threshold T4 to include only completely burnt pixels. Following the approach discussed in section 'Setting the thresholds' under 'Asessing the performance of the burnt area indices in detecting burnt and unburnt pixels', we set TBI ≤ the 95th percentile value of completely burnt pixels and BAIS2 ≥ the 5th percentile value of completely burnt pixels, as shown in Figure 5. We then applied this threshold to the test dataset to analyse its performance in detecting completely burnt fields.

Figure 5. Threshold T4 includes only completely burnt pixels

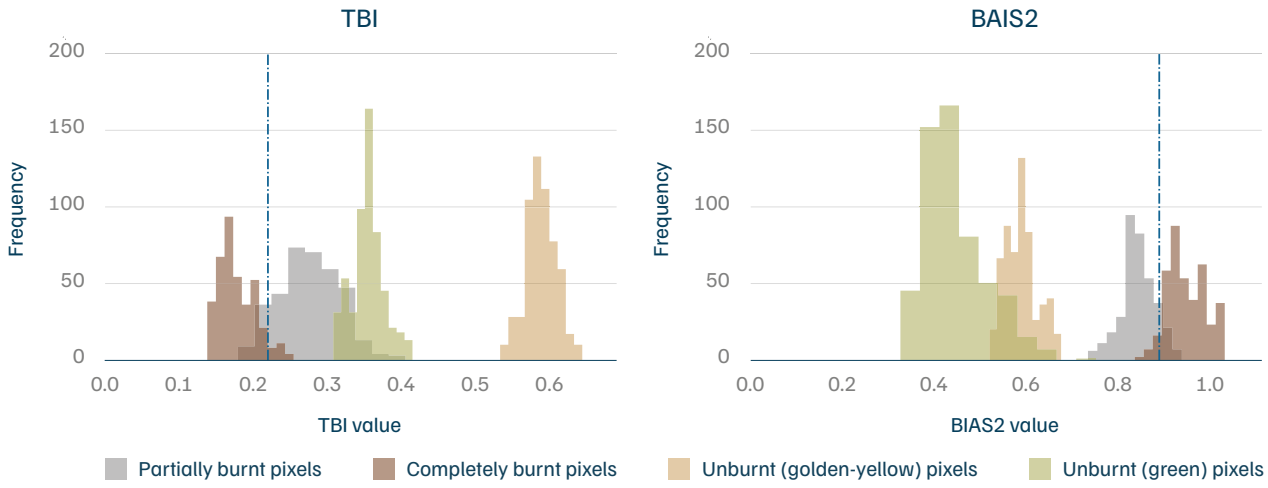

Source: Authors' analysis

Figure 6. An overview of the data and methodology

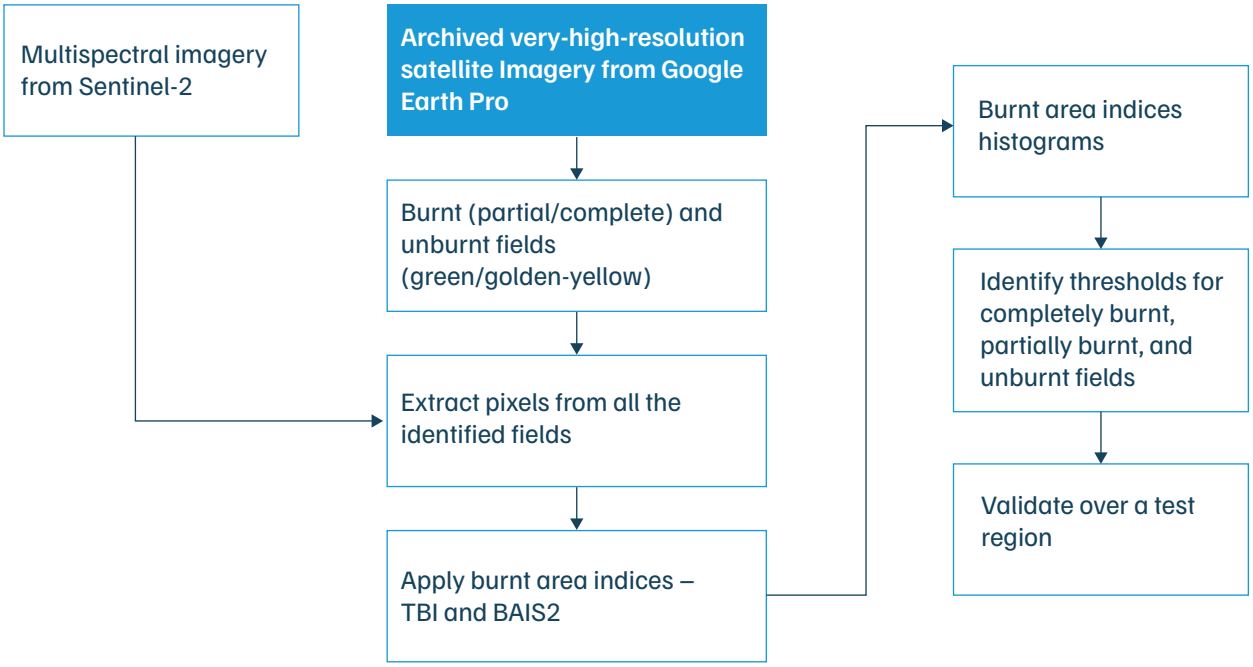

Source: Authors' analysis

Figure 7. An overview of the methodology adopted for differentiating partially and completely burnt fields

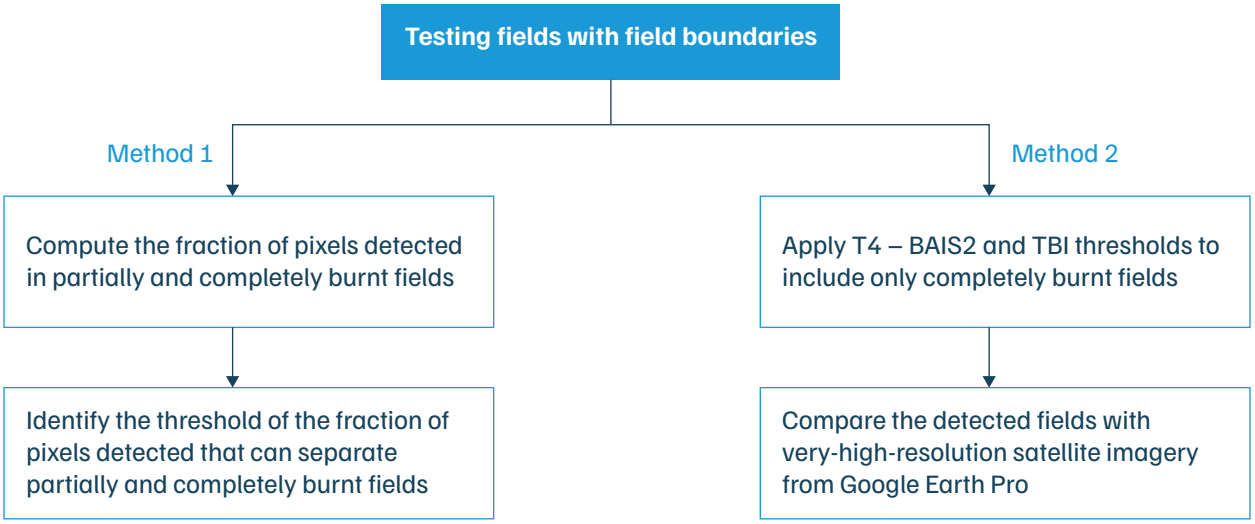

Source: Authors' analysis

3. Results and discussion

In this section, we present the extent to which the satellite-borne sensors capture CRB incidents. We also present performance of our burnt area algorithm in detecting burnt fields and the ability of our algorithm to differentiate between partially and completely burnt fields.

3.1 Satellite-borne sensors are unable to detect all farm fires

Our analysis of very-high-resolution satellite imagery over a sample area of 74 sq km in Sangrur shows that 169 fields that were unburnt on 9 November appeared burnt on 10 November. However, the VIIRS overpasses on these two days detected only seven fires in this region, while MODIS detected none. This suggests that most farm fire incidents went undetected by satellites. The fire radiative power (FRP) values of the detected fires ranged from 2.8 to 7.1. Figure 8 illustrates the burnt fields identified using very-high-resolution satellite imagery on 9 and 10 November 2020, along with the subset detected by VIIRS on either of these two days.

Figure 8. Satellite-borne sensors such as the Visible Infrared Imaging Radiometer Suite (VIIRS) may detect only a few farm fire incidents

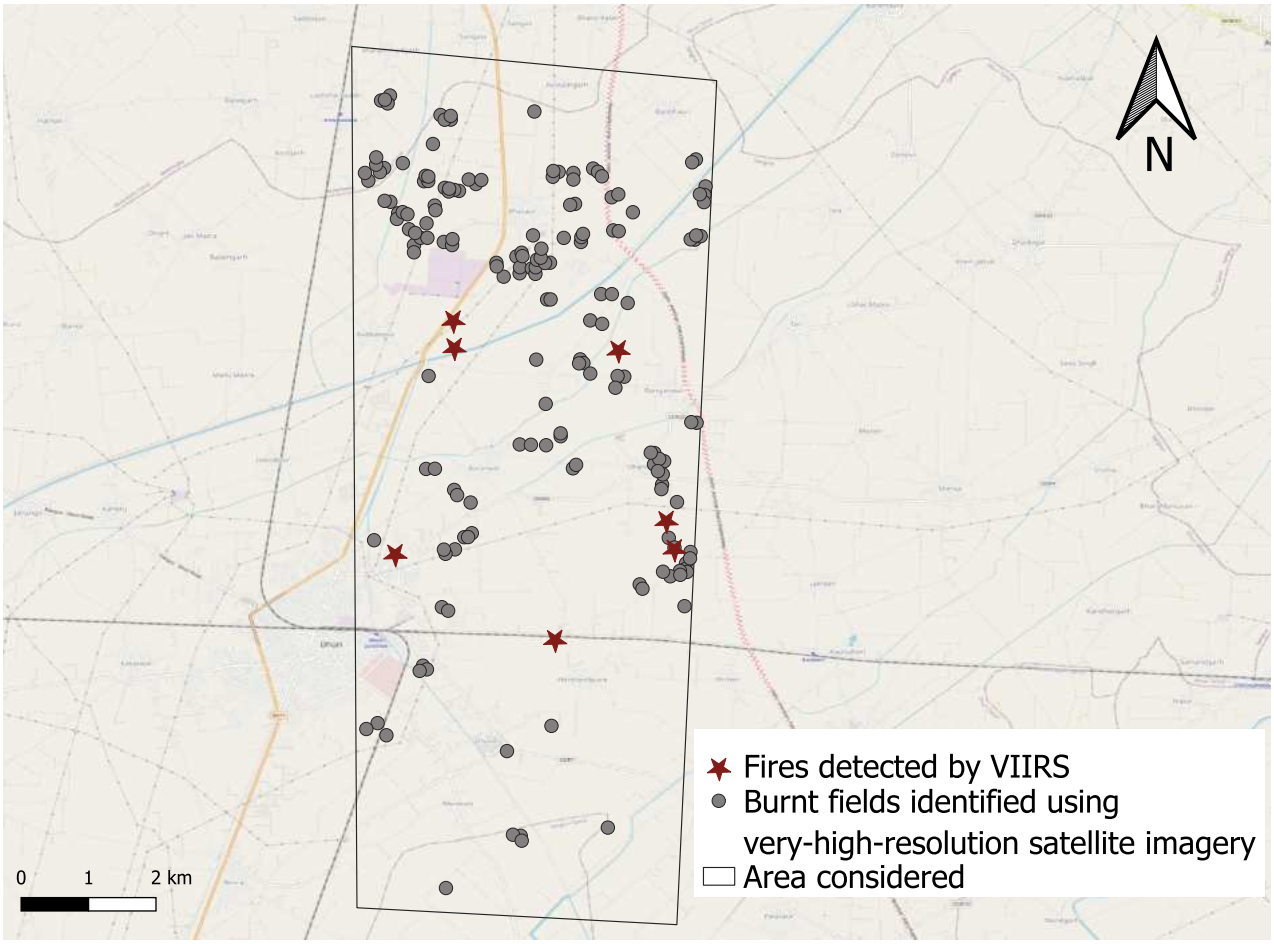

Source: Authors' analysis

3.2 A combination of Burnt Area Index for Sentinel-2 (BAIS2) and Tasseled Cap Brightness Index (TBI) separates unburnt and burnt fields accurately

We applied the thresholds T1, T2, and T3 identified in the section 'Setting the thresholds' under 'Asessing the performance of the burnt area indices in detecting burnt and unburnt pixels', to the test fields and analysed their ability to detect burnt fields. First, we determined the number of fields detected after applying these thresholds. We marked a field as 'detected' if the algorithm detects at least one pixel (~100 sq m) within the field. Table 5 presents the number of fields detected corresponding to each threshold.

Table 5. Threshold T3 performs the best with the least number of misclassifications

	Number of fields detected applying T1	Number of fields detected applying T2	Number of fields detected applying T3
Burnt fields	270 out of 287	284 out of 287	262 out of 287
Unburnt fields	23 out of 95	92 out of 95	13 out of 95

Source: Authors' analysis

Threshold T1 correctly detected 270 of 287 burnt fields but misclassified 23 of 95 unburnt fields as burnt. T2 detected 284 of 287 burnt fields but misclassified 92 of 95 unburnt fields as burnt. In contrast, T3 correctly classified 262 of 287 burnt fields and misclassified only 13 unburnt fields as burnt.

As Table 5 shows, the algorithm with T3 performed reasonably well in classifying burnt and unburnt fields. However, accurate computation of burnt area also requires the correct detection of individual burnt pixels. To assess the ability of these thresholds to detect burnt pixels accurately, we applied thresholds T1, T2, and T3 to the test fields; this comprised a total of 13,146 burnt pixels and 8,382 unburnt pixels. Tables 6 and 7 present the confusion matrices and performance metrics for each threshold.

Table 6. A combination of BAIS2 and TBI gives the least number of false positives

T1		
	True	False
True	8,374	163
False	4,772	8,219

T2		
	True	False
True	12,002	6,416
False	1,144	1,966

T3		
	True	False
True	7,808	52
False	5,338	8,330

Source: Authors' analysis

Table 7. T1 performs better in most metrics, but T3 gives the fewest false positives

Metric	T1	T2	T3
Accuracy	0.77	0.65	0.75
True positive rate (TPR)	0.64	0.91	0.59
False positive rate (FPR)	0.019	0.77	.006
False negative rate (FNR)	0.36	0.087	0.406
F1 score	0.77	0.76	0.743
Matthews correlation coefficient (MCC)	0.62	0.20	0.60
Cohen's kappa (k)	0.56	0.17	0.53

Source: Authors' analysis

Applying threshold T1 resulted in 8,374 true positives with a TPR of 0.64. It achieved the highest accuracy of 0.77, an MCC of 0.62, and a Cohen's kappa of 0.56. It also yielded 163 false positives, corresponding to an FPR of 0.019. The FNR of T1 was the lowest at 0.36. T1 also yielded the highest F1 score at 0.77, indicating the algorithm's ability to detect burnt pixels accurately.

T2 recorded the highest number of true positives at 12,002, with a TPR of 0.91. However, its accuracy, MCC, and Cohen's kappa were the lowest at 0.65, 0.20, and 0.17, respectively. False positives were also the highest at 6,416, with an FPR of 0.77. While its FNR was the lowest at 0.087, its F1 score was 0.76, comparable to T1.

T3 yielded 7,808 true positives and the fewest false positives at 52. It achieved an accuracy of 0.75, MCC of 0.60, and Cohen's kappa of 0.53–all comparable to T1. However, T3 had the lowest F1 score at 0.74, a TPR comparable to T1 (0.59), and an FNR 0.406 higher than that of T1. The FPR of T3 was the lowest at 0.006.

Thus, to optimise burnt area calculation with the least possible false detections, we set the algorithm threshold as the combination of BAIS2 >= 5th percentile of partially burnt pixels and TBI <= 95th percentile of partially burnt pixels. The threshold combination from the training dataset is TBI <= 0.34 and BAIS2 >= 0.78. We observed that while T3 produced the lowest FPR, T1 outperformed T3 on all other metrics. Moreover, the FPR of T1 is only about 0.019. This indicates that T1 can also serve as a reliable threshold for detecting burnt areas.

3.3 Differentiating between partially and completely burnt fields is difficult

We assessed the ability of the two methods described in the section 'Assessing the ability of the algorithm to differentiate between partially and completely burnt fields' to differentiate between partially and completely burnt fields. We provide a detailed explanation of the performance of both methods in differentiating these fields in the following section.

Method 1

In this method, we calculated the percentage of pixels detected in each field after applying T3. Figure 9 presents the box plot of the percentage of pixels detected in partially and completely burnt fields under this threshold. The median[3] percentage of burnt pixels detected in completely burnt fields was 76 per cent, whereas it was 55 per cent in the case of partially burnt fields. However, there was an overlap in the values of the percentage of pixels detected in the two types of fields. This suggests that distinguishing between partially and completely burnt fields based on the percentage of pixels detected in a field is challenging.

To assess the extent to which the separation between these fields is possible, we computed the number of fields detected upon applying different thresholds of detected pixel percentage. We set thresholds of the percentage of pixels detected in a field, starting from the 5th percentile of the percentage of pixels detected in completely burnt fields.

3. The mean and standard deviation of the percentage of pixels detected in completely burnt fields are 68 per cent and 27 per cent, respectively, whereas they are 51 per cent and 31 per cent, respectively, for partially burnt fields.

Figure 9. The median percentage of burnt pixels detected in completely burnt fields is 76% and that in partially burnt fields is 55%

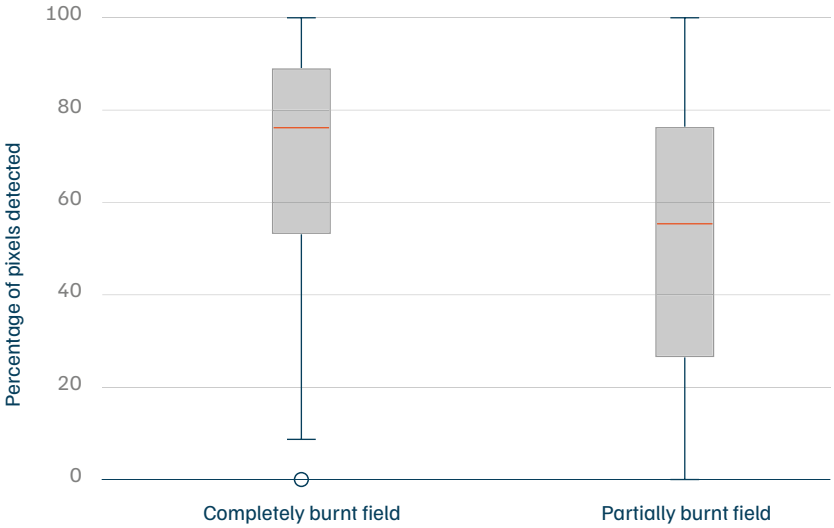

Source: Authors' analysis

To analyse the threshold at which the algorithm maximises the detection of completely burnt fields and minimises that of partially burnt fields, we varied the thresholds, as presented in Table 8.

Table 8. Number of fields detected under different percentage detection thresholds

	If the percentage of pixels detected in a field > Kth percentile of the percentage of pixels detected in completely burnt fields									
	K = 5	**K = 10**	**K = 15**	**K = 20**	**K = 25**	**K = 30**	**K = 40**	**K = 50**	**K = 75**	**K = 90**
Number of completely burnt fields classified as completely burnt (out of 72)	68	63	61	57	55	50	43	36	20	8
Number of partially burnt classified as completely burnt fields (out of 190)	153	140	128	106	98	90	76	48	20	10

Source: Authors' analysis

From Table 8, we observe that a threshold of the 5th percentile correctly classified 68 of 72 completely burnt fields, but also misclassified 153 of 190 partially burnt fields as completely burnt fields. The algorithm's misclassification of partially burnt fields decreased as the detection threshold percentage increased. A threshold of the 25th percentile classified 76 per cent of completely burnt fields correctly, while misclassifying 51 per cent of partially burnt fields as completely burnt. While it only detects 20 of 190 partially burnt fields at the 75th percentile detection threshold, it only detects 20 of 72 completely burnt fields.

To identify an optimum threshold value, we plotted the receiver operating characteristic (ROC) curve, which shows the relationship between the probability of detection (POD)[4] and false alarm ratio (FAR)[5] (Figure 10). We computed POD and FAR for all thresholds in Table 8, but none yielded an optimum threshold with a high POD and low FAR. For instance, when the percentage of pixels detected in a completely burnt field exceeded the 40th percentile of the percentage of pixels detected in the completely burnt fields (K = 40), POD was 0.6 but with an FAR of 0.4.

Figure 10. No threshold resulted in an optimum detection with a high probability of detection and a low false alarm ratio

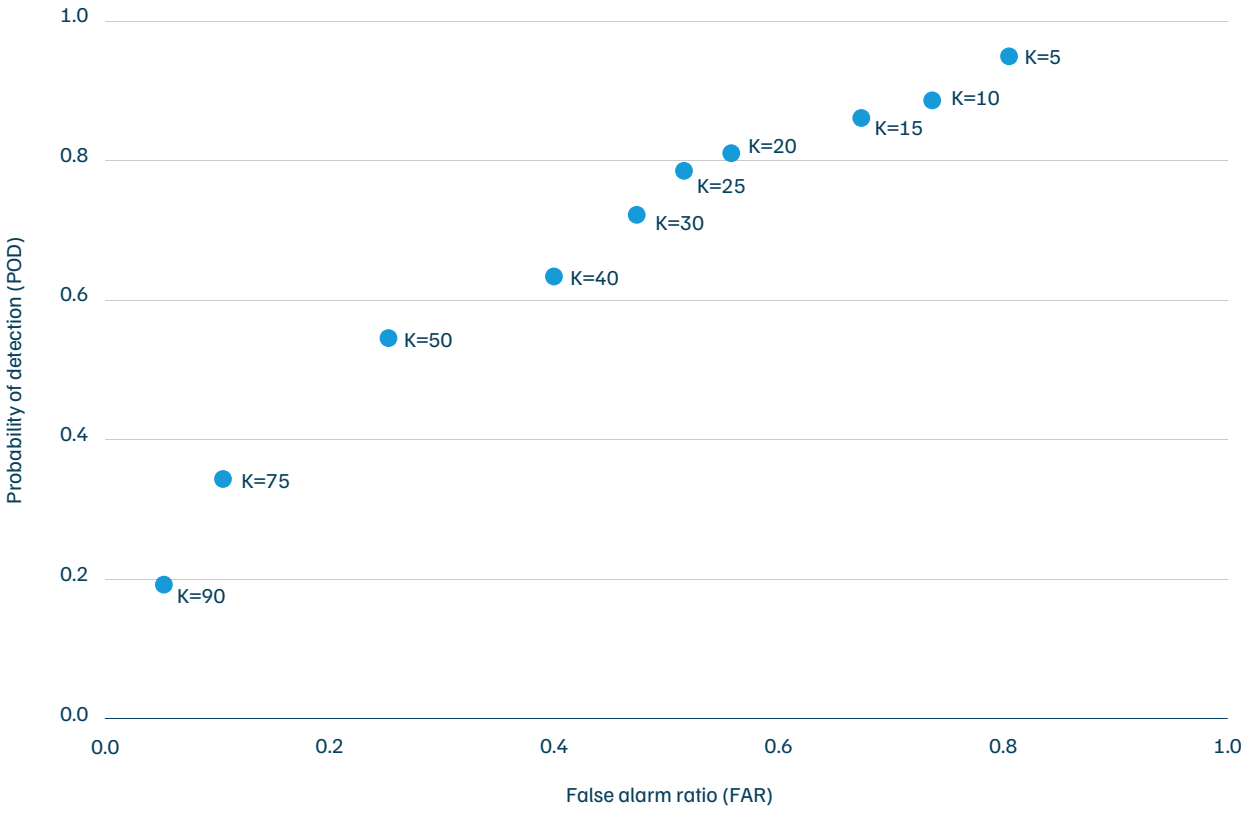

Source: Authors' analysis

Method 2

In this method, we applied threshold T4, designed to identify only completely burnt fields, to distinguish between the two field types. As shown in Section 3.2, T1 (only BAIS2) and T3 (a combination of BAIS2 and TBI) performed well in detecting burnt fields, with T3 yielding the fewest false positives. Therefore, to minimise false positives, we designed T4 as a combination of BAIS2 and TBI. From the training dataset, T4 is a combination of TBI <= 0.22 and BAIS2 >= 0.89. Table 9 summarises this threshold. We applied this threshold to the test fields and computed the number of completely burnt fields detected upon applying T4.

4. POD = TP/(FN + TP)
5. FAR = FP/(TN + FP)

Table 9. The value of threshold T4 is BAIS2 >= 0.89 and TBI <= 0.22

Threshold	Threshold description	Threshold value
T4	BAIS2 >= 5th percentile value of completely burnt pixels, and TBI <= 95th percentile value of completely burnt pixels	BAIS2 >= 0.89 and TBI <= 0.22

Source: Authors' analysis

Upon applying T4, the algorithm could only detect 39 per cent of completely burnt fields. It also misclassified 15 per cent of partially burnt fields as completely burnt fields. Table 10 shows the number of fields detected after applying T4. We followed the same methodology to analyse the performance of MIRBI in detecting burnt area and its ability to differentiate between partially burnt and completely burnt fields. Annexure 4 includes the results.

Table 10. Threshold T4 could only detect 39 per cent of completely burnt fields

Category of field	Number of fields detected upon applying T4
Partially burnt	30 out of 190
Completely burnt	28 out of 72

Source: Authors' analysis

We conclude that differentiating between completely burnt fields and partially burnt fields is challenging. However, given the algorithm's ability to detect burnt fields with an accuracy of 75 per cent, we propose a methodology to compute burnt area using a combination of BAIS2 and TBI for a region in India. Figure 11 illustrates the detailed methodology for computing the burnt area in this region.

Figure 11. An overview of the proposed methodology to compute the burnt area over a region

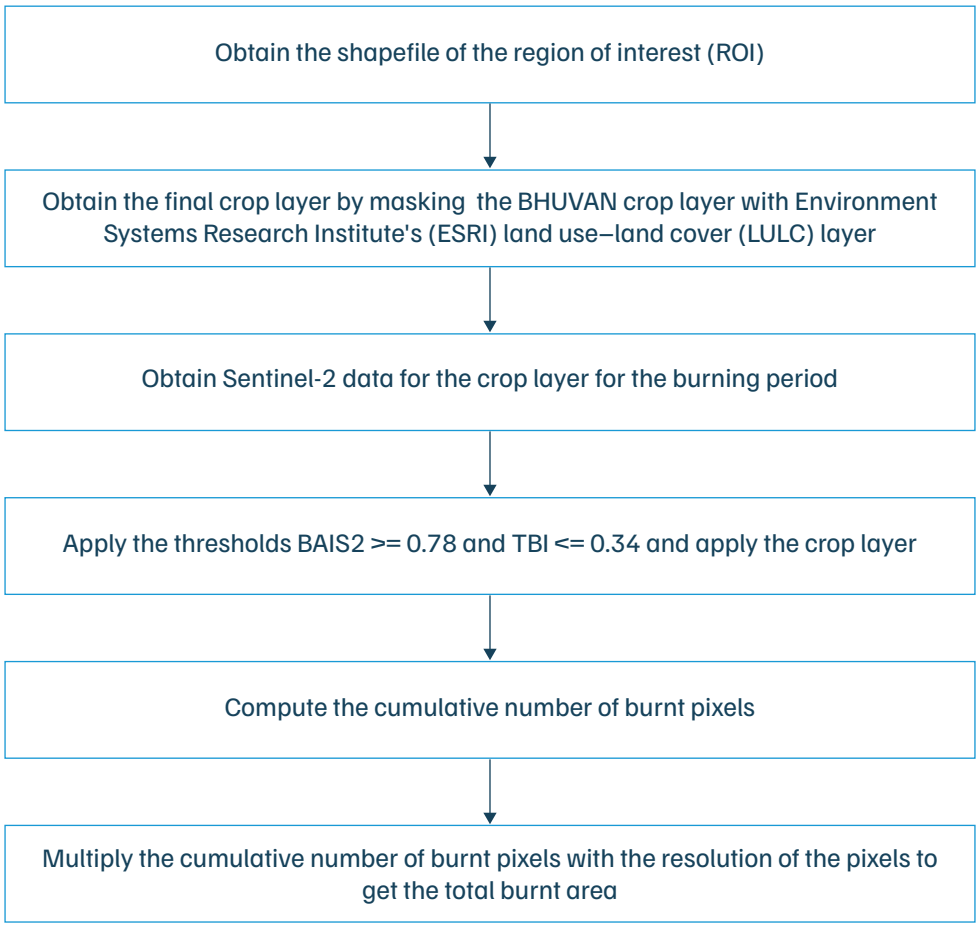

Source: Authors' analysis

We obtained the land use–land cover (LULC) layer from ISRO's BHUVAN portal. From the LULC dataset, we selected the 'double crop' and 'kharif crop' layers for the crop layer. Using LULC data from the Environment Systems Research Institute (ESRI), we removed all land use classes except 'Crop' (i.e., 'Water', 'Trees', 'Flooded Vegetation', 'Bare Ground', 'Snow/Ice', 'Rangeland', 'Clouds' and 'Built Area') to create an accurate crop layer for our region of interest (ROI). We then obtained Sentinel-2 data for the ROI during the burning period (15 September–30 November). We applied the burnt area threshold T3 (BAIS2 >= 0.78 and TBI <= 0.34) over the Sentinel-2 layer along with the crop layer. We computed the burnt area on all satellite pass dates separately during the considered time period. To avoid double-counting, pixels already marked as detected were excluded from subsequent passes. We computed the cumulative number of pixels detected over the considered time period, as well as the total burnt area, by multiplying the number of pixels by the area of a single pixel.

We applied the burnt area algorithm to Punjab during the kharif burning period from 2019 to 2024. Annexure 2 presents the burnt area obtained for different districts across this period. We also compared burnt area estimates for three districts–Amritsar, Barnala, and Tarn Taran–with VIIRS fire counts detected during the same burning period. Annexure 3 provides the results and details of changes in burnt area for these districts between 2019 and 2024.

4. Limitations

The burnt area algorithm performs reasonably well in detecting burnt fields and pixels. However, the current study has certain limitations.

4.1 Loss of data due to the low temporal resolution of Sentinel-2

The Sentinel-2 constellation passes over a given region every five days. Therefore, the satellites do not capture the fields that are burnt and managed within the five days between two successive overpasses. For instance, Figure 12 illustrates very high-resolution images of a field managed between 26 and 29 October 2021. Critically, while the Sentinel-2 passes over the area were on 24 and 29 October 2021, a burn occurring on 25, 26, or 27 October would likely be undetectable by the burnt area algorithm run on the 29 October imagery if the field was managed quickly afterwards.

Figure 12. Farmers might burn and manage the fields within five days, and satellites may miss capturing such fields

a. Very-high-resolution image captured on 26 October 2021

b. Very-high-resolution image captured on 29 October 2021

Source: Google Earth Pro

4.2 Loss of data due to clouds and smoke

Data availability from satellites depends on atmospheric conditions. Clouds and shadows of smoke plumes result in a loss of surface reflectance data from Sentinel-2 (Pinto et al. 2021). If a burnt field goes uncaptured on the day of a satellite pass, it is unlikely to remain unmanaged by the time of the next pass. Therefore, such fields go uncaptured in burnt area estimates.

4.3 Exclusion of managed fields under unburnt fields

We excluded fields managed using CRM machinery from the unburnt category, as they cannot be reliably identified using very-high-resolution imagery. Identifying and marking such fields as managed would require ground-based surveys.

4.4 Detection of irrigated fields

The algorithm occasionally detected a few irrigated fields as burnt, as they appear black in the satellite imagery. To examine this, we identified a few fields with water flow streaks clearly visible in the very-high-resolution imagery. We computed TBI and BAIS2 for these fields and assessed whether the indices could distinguish between irrigated fields and burnt fields. BAIS2 and TBI failed to differentiate between burnt and irrigated fields, as shown in Figure 13. Therefore, the algorithm might misclassify a few irrigated fields as burnt. However, information on the irrigation schedule in a region could help avoid this misclassification.

Figure 13. BAIS2 and TBI do not separate irrigated fields and burnt fields

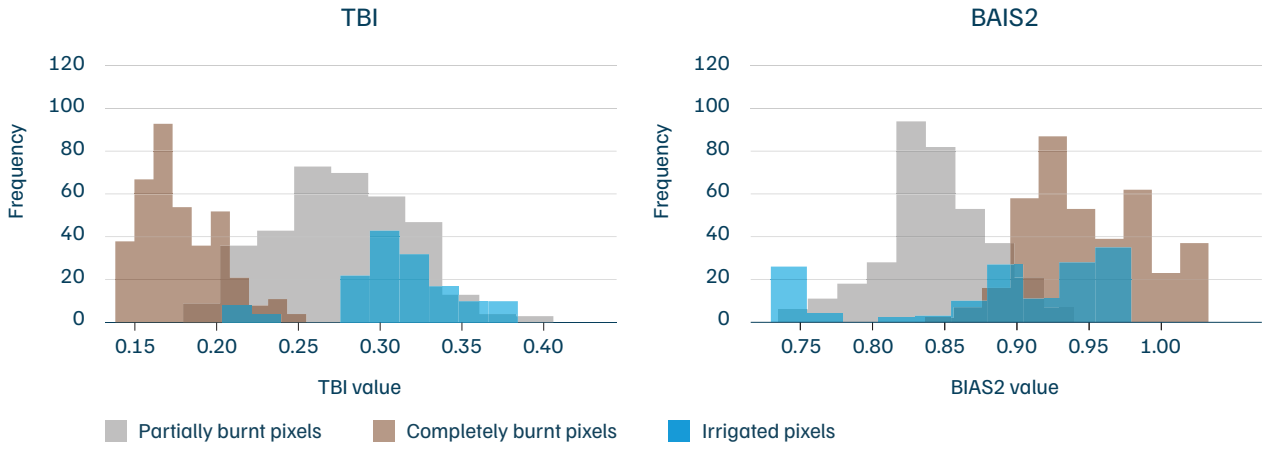

Source: Authors' analysis

4.5 Differentiating between partially and completely burnt fields

In some cases, differentiating between completely and partially burnt fields was challenging, even in very-high-resolution imagery. While some fields clearly appeared completely burnt, others showed a mix where a portion could be completely burnt, while the rest appeared partially burnt. Farmers burn in various ways, which leads to differences in the appearance of the fields. Figure 14 presents images of fields that were indistinguishable. Therefore, we only included fields that were clearly identifiable as partially burnt or completely burnt in our training dataset. We also acknowledge the possibility of missing a few dates where very-high-resolution satellite imagery and Sentinel-2 passes coincided, considering the manual effort required to match them.

Figure 14. Distinguishing between partially and completely burnt fields is difficult in some cases, even in very-high-resolution imagery

Source: Google Earth Pro

5. Conclusion and way forward

Our analysis of very-high-resolution satellite imagery from two consecutive days in November 2020, covering a 74 sq km area in Punjab, suggests that satellite-borne sensors may underreport farm fire incidents. The VIIRS sensor onboard SUOMI-NPP detected only 7 fire incidents, whereas 169 fields appeared burnt. This demonstrates that fire counts are not a reliable metric for monitoring the extent of CRB. An alternate approach is to compute the burnt area. We analysed the performance of two burnt area indices, BAIS2 and TBI, in distinguishing burnt from unburnt fields. Tested both individually and in combination, the indices performed best when combined, achieving an accuracy of 75 per cent in detecting burnt pixels with an FPR of 0.006.

We also examined the ability of burnt area indices to differentiate between partially and completely burnt fields. We applied two methods. Method 1 relies on the hypothesis that the percentage of burnt pixels in partially burnt fields will be lower than in completely burnt fields. However, this method could not reliably distinguish between the two types of fields. The median percentage of pixels detected was 55 per cent in partially burnt fields and 76 per cent in completely burnt fields. Method 2 was applying a combination of BAIS2 and TBI, intended to detect only completely burnt pixels, but it could not separate the two types of fields and only detected 39 per cent of completely burnt fields. We conclude that while burnt area algorithms can detect burnt pixels with reasonable accuracy, differentiating between completely and partially burnt fields remains a challenge. Based on our findings, we recommend the following:

- **Central and state government bodies should consider using very-high-resolution satellite imagery to monitor CRB alongside the current methods**. Given the challenges associated with burnt area algorithms and fire count–based methods in identifying the extent of partial and complete burning, using very-high-resolution imagery is currently the only reliable alternative. Commercial satellite imagery providers, such as Maxar Technologies and Planet Labs, offer daily very-high-resolution images. Therefore, central and state government bodies—such as the CAQM, agriculture departments, and remote-sensing centres—could use such data to monitor CRB alongside current methods. However, very-high-resolution satellite imagery comes at a prohibitive cost. To reduce procurement costs, government bodies could choose a sample time period during the season for monitoring instead of procuring data for the entire burning season.

- **The Indian Institute of Tropical Meteorology (IITM)/India Meteorological Department (IMD) should include the emission estimates from burnt area, along with those from fire counts, in their EIs**. India's AQEWS provides forecasts of particulate matter and other pollutants days in advance. Currently, the EIs behind this system rely on fire counts to estimate CRB emissions (Govardhan et al. 2024). However, given the uncertainties associated with fire counts, such as the underestimation of fires and the occurrence of post-overpass burning, errors will occur in the emission estimates.

- **India should operate its own constellation of satellites for environmental monitoring in tandem with the Sentinel-2 constellation**. Sentinel-2's five-day revisit time limits continuous CRB monitoring. A dedicated constellation with comparable performance would increase temporal resolution and provide more reliable CRB data, eliminating the current five-day delay. ISRO has already demonstrated its capability in designing and launching satellites for various earth observation purposes through its Earth Observation Satellites (EOS) from the Oceansat series. Beyond CRB, such a constellation would support several objectives, including monitoring wildfires, deforestation, and damage caused by climate-related disasters.

Our analysis shows that fire counts are not a reliable metric for monitoring CRB. While burnt area serves as an alternative, it is challenging to differentiate between partailly and completely burnt fields using burnt area indices. It also comes with limitations like coarse temporal resolution and loss of data due to clouds, among others. Accurate estimation of CRB will not only improve the performance of air quality models providing air quality forecasts but also help assess the effectiveness of CRB mitigation policies. While the use of commercially available very-high-resolution imagery will help improve CRB monitoring, India's long-term priority should be to invest in expanding its satellite programme to have additional satellites which would support CRB monitoring along with other environment, agriculture and climate-related applications.

Annexures

Annexure 1

TBI uses bands in the visual spectrum (B2, B3, B4), a near-infrared band (B8), shortwave-infrared short-reflectance band (B11), and shortwave-infrared long-reflectance band (B12), whereas BAIS2 uses red-edge bands (B6, B7, B8A), B12, and B4. The resolution of the bands in the visual spectrum and the near-infrared band is 10 metres and that of the others is 20 metres. Table A1 explains the formulae used for computing TBI and BAIS2 using Sentinel-2 band values (Deshpande et al. 2022). Table A2 presents the wavelength of Sentinel-2 bands.

Table A1. Formulae used for computing BAIS2 and TBI

Burnt area index	Formula
BAIS2	(1-√((B6×B7×B8)/B4))×((B12-B8A)/√(B12+B8A)+1)
TBI	((0.3510×B02)+(0.3813×B03)+(0.3437×B04)+(0.7196×B08)+(0.2396×B11)+(0.1949×B12))

Source: Authors' compilation

Table A2. Sentinel-2 bands and wavelengths

Band number	Central wavelength (nm)
1	443
2	490
3	560
4	665
5	705
6	740
7	783
8	842
8a	865
9	940
10	1,375
11	1,610
12	2,190

Source: Authors' compilation

Annexure 2

We computed the district-wise burnt area using our algorithm between 15 September and 30 November from 2019 to 2024.

Table A3. Burnt area in the districts of Punjab

	Burnt Area (sq km)					
District	**2019**	**2020**	**2021**	**2022**	**2023**	**2024**
Amritsar	1,250.325	1,409.766	1,428.142	1,427.163	1,184.554	1,250.493
Barnala	969.0043	779.8613	1,085.774	1,054.603	709.1857	954.3842
Bathinda	1,744.342	1,628.304	1,931.857	2,109.157	1,389.638	1,885.618
Faridkot	1,055.357	985.4276	1,081.012	1,066.604	779.0258	994.0018
Fatehgarh Sahib	671.3433	693.9028	801.3894	774.3122	733.9899	750.2244
Fazilka	1,093.118	1,072.911	1,059.646	1,133.223	772.3494	1,049.603
Firozpur	1,763.679	1,698.194	1,778.036	1,771.152	1,417.506	1,511.943
Gurdaspur	1,247.218	1,127.224	1,321.527	1,212.09	1,083.142	1,106.777
Hoshiarpur	461.3704	636.7012	625.4784	599.7605	509.3772	510.8112
Jalandhar	1,406.895	1,158.34	1,514.923	1,432.474	1,100.413	1,072.771
Kapurthala	884.9969	778.4859	957.0267	912.4809	839.8714	672.4907
Ludhiana	1,827.72	1,553.548	2,265.378	2,096.804	1,612.801	1,814.703
Malerkotla	373.8945	266.2054	477.8027	462.5671	410.6653	439.4839
Mansa	1,118.307	1,072.992	1,248.634	1,395.011	852.5471	1,284.869
Moga	1,456.124	1,388.36	1,733.384	1,590.029	986.2575	1,399.364
Pathankot	133.0264	173.8436	169.4441	152.8192	160.5541	151.0572
Patiala	1,777.035	1,904.412	2,085.746	1,970.835	1,738.891	2,043.011
Rupnagar	358.9448	363.2317	425.8327	365.8831	280.4489	329.7422
Sangrur	1,929.662	1,804.811	2,265.006	2,177.061	1,686.038	2,074.9
Sas Nagar	156.4162	250.9272	205.955	196.045	158.6877	224.4244
Shaheed Bhagat Singh	403.5248	317.3594	464.2934	425.7374	373.688	370.6063
Sri Muktsar Sahib	1,648.582	1,474.515	1,638.912	1,717.28	1,132.144	1,466.951
Tarn Taran	1,513.832	1,528.814	1,554.639	1,587.564	1,145.289	1,214.749
Total	**25,244.72**	**24,068.14**	**28,119.84**	**27,630.66**	**21,057.06**	**24,572.98**

Source: Authors' compilation

Note: We used the 2023 crop layer for computing the burnt area for 2024, as the 2024 crop layer was unavailable.

We observed that the total burnt area peaked in kharif 2021, reaching up to 28,119 sq km. It slightly dropped to 27,630 sq km in kharif 2022 and further dropped to 21,057 sq km in kharif 2023. However, it increased by 3,516 sq km in 2024 compared to the previous year.

Annexure 3

We compare the change in burnt area computed using our algorithm with that of the fire counts observed by the VIIRS instrument over three districts in Punjab – Amritsar, Barnala, and Tarn Taran – during the kharif season (15 September–30 November) over the last six years.

We identified Sentinel-2 pass days during the burning period over Punjab for each year. We then calculated the cumulative freshly burnt area during the five days between the satellite overpass dates using our algorithm. Similarly, we obtained the cumulative VIIRS fire counts during these days. We compared the cumulative fire counts with the cumulative burnt area. We fitted a line to establish the relationship between fire counts and burnt area on a year-by-year basis. Using the equations derived for 2020 and 2023, we calculated the number of fire counts in 2024 for the selected districts, based on their burnt area data. Figure A1 illustrates the relation between burnt area and fire counts for these districts.

From Figure A1, we observe a change in the relationship between burnt area and fire counts over the past five years. In Amritsar, the burnt area remained around 1,200–1,400 sq km between 2019 and 2024. However, the number of fire counts declined from 2,707 in 2020 to 549 in 2024. Similarly, in Barnala, the slope of the burnt area versus fire counts line was 6.5 in 2020 but dropped to 0.22 in 2024. While the burnt area in 2024 increased by 22 per cent compared to 2020, fire counts fell by 95 per cent over the same period. In Tarn Taran, the number of fires in 2024 decreased by 85 per cent compared to 2020, while the burnt area declined only by 20 per cent. These findings suggest that the number of fire incidents occurring after the satellite overpass time may have increased in 2024, resulting in a drastic change in the relationship between burnt area and fire counts in 2024. The extent of this change differs by district. For instance, based on past trends, Barnala could have recorded between 3,000 and 6,000 fire counts in 2024, compared to the 228 observed.

Figure A1. Number of fire incidents after the satellite pass increased in 2024

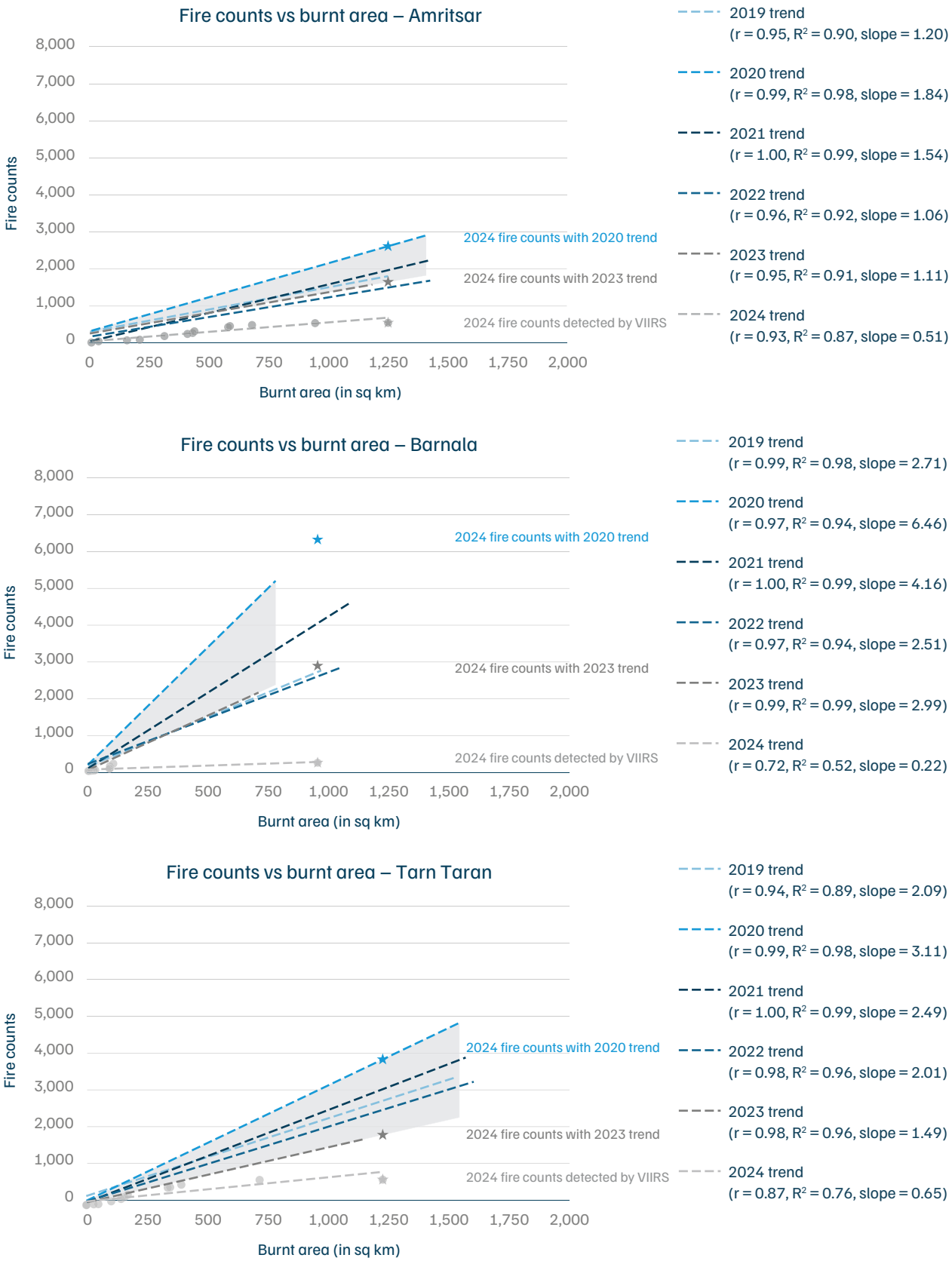

Source: Authors' analysis

Annexure 4

We assessed the performance of the MIRBI index following the same methodology adopted in Section 2. We computed the MIRBI of partially burnt, completely burnt, green unburnt, and golden-yellow unburnt fields in the training dataset. Thereafter, we plotted a histogram of the MIRBI obtained for different field types. Figure A2 displays the obtained histogram.

Figure A2. Mid-Infrared Burn Index can potentially differentiate between burnt and unburnt pixels

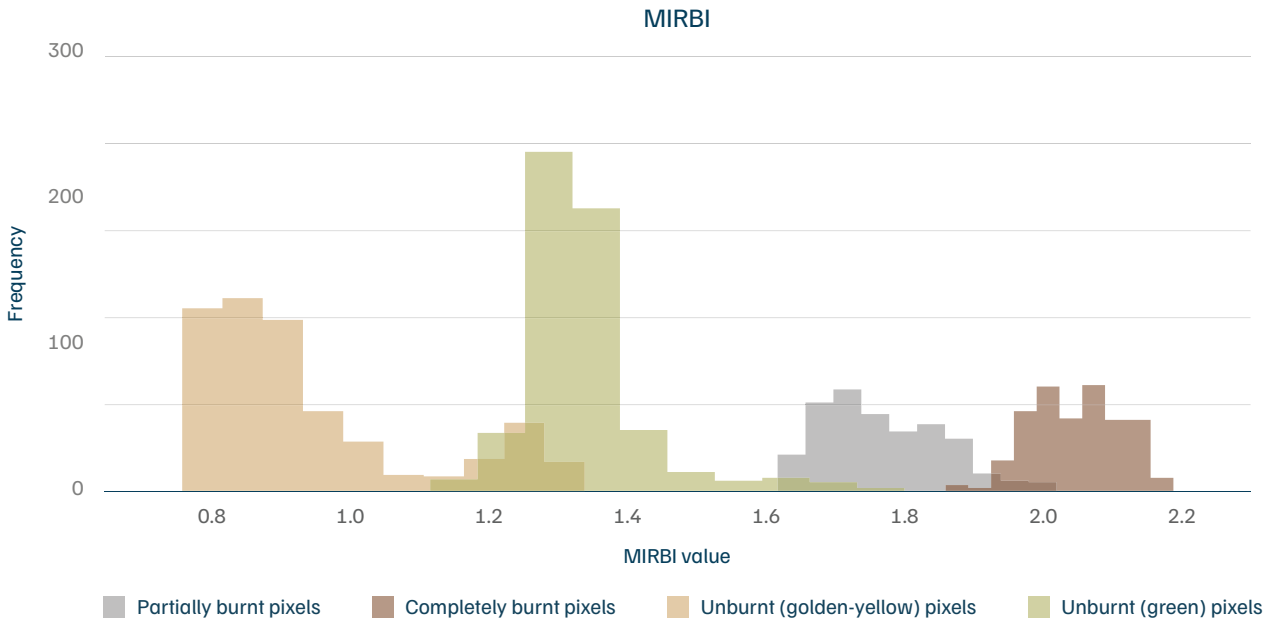

Source: Authors' analysis

The histogram in Figure A2 displays that MIRBI can also potentially differentiate between burnt and unburnt fields. Therefore, to assess MIRBI's ability to detect burnt and unburnt fields, we defined threshold T5 as MIRBI >= 5th percentile value of partially burnt fields. From the training dataset, this corresponded to MIRBI >= 1.65. Table A4 summarises threshold T5.

Table A4. T5 is set at greater than or equal to the 5th percentile of partially burnt pixels

Threshold	Threshold description	Threshold value
T5	MIRBI >= 5th percentile value of partially burnt pixels	MIRBI >= 1.65

Source: Authors' analysis

We applied this threshold to the testing fields used in this study. Table A5 displays the number of fields detected upon applying T5.

Table A5. T5 detects burnt fields but has 80 per cent misclassifications

	Number of fields detected applying T5 threshold
Burnt fields	286 out of 287
Unburnt fields	77 out of 95

Source: Authors' analysis

We observed that T5 correctly detected 286 of 287 burnt fields but also misclassified 77 of 95 unburnt fields (80 per cent) as burnt. To assess performance at the pixel level, we computed the confusion matrix (Table 3) and the corresponding performance metrics. Tables A6 and A7 present the confusion matrix and performance metrics obtained when T5 was applied to the test fields.

Table A6. The confusion matrix obtained for T5

		Observed	
		True	False
Detected	True	12,466	5,726
	False	700	2,656

Source: Authors' analysis

Table A7. Performance metrics of T5

Metric	T5
Accuracy	0.701
True positive rate (TPR)	0.95
False positive rate (FPR)	0.683
False negative rate (FNR)	0.053

Source: Authors' analysis

We observed that T5 could detect burnt pixels with an accuracy of 0.7. It has a TPR of 0.95. While the FNR of T5 is low at 0.053, it has a high FPR of 0.68, compared with 0.019 for T1 and 0.006 for T3. We also assessed the ability of MIRBI to differentiate between partially burnt and completely burnt fields following the methodology provided in Section 2.

Method 1

We applied T5 to the test fields. We then computed the percentage of pixels detected in completely burnt and partially burnt fields. Figure A3 presents the percentage of pixels detected in each field type.

Figure A3. The median percentage of pixels detected in partially and completely burnt fields is 100 per cent

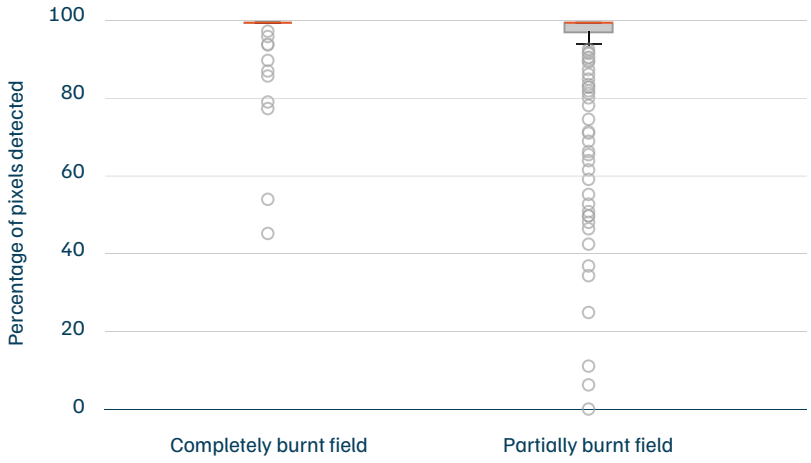

Source: Authors' analysis

We observed that all quartile values (25th, 50th, and 75th percentiles) of the percentage of pixels detected in both partially and completely burnt fields were 100 per cent. This made it difficult to select a threshold percentage of pixels detected in a field to differentiate between two field types. We therefore conclude that Method 1 fails to differentiate between partially and completely burnt fields.

Method 2

In Method 2, we assessed the performance of MIRBI in detecting only completely burnt areas. We defined threshold T6 as MIRBI >= 5th percentile value of completely burnt pixels to include only completely burnt fields. Table A8 summarises threshold T6.

Table A8. Threshold T6 only includes completely burnt pixels

Threshold	Threshold description	Threshold value
T6	MIRBI>=5th percentile value of completely burnt pixels	MIRBI >= 1.95

Source: Authors' analysis

We computed the number of partially and completely burnt fields detected after applying T6. Table A9 summarises the results obtained.

Table A9. T6 could detect 74 per cent of completely burnt fields but also misclassified around 74 per cent of partially burnt fields

Category of field	Number of fields detected upon applying T6
Partially burnt	142 out of 190
Completely burnt	53 out of 72

Source: Authors' analysis

We observed that T6 detected around 74 per cent of completely burnt fields. However, it also misclassified around 75 per cent of partially burnt fields as completely burnt. This implies that the index is more unreliable than a combination of BAIS2 and TBI for differentiating between partially burnt and completely burnt fields.

Acronyms

AQEWS	Air Quality Early Warning System
BAI	Burn Area Index
BAIS2	Burnt Area Index for Sentinel-2
CAQM	Commission for Air Quality Management in National Capital Region and Adjoining Areas
CBG	compressed biogas
CHCs	custom hiring centres
CO	carbon monoxide
CO2	carbon dioxide
CRB	crop residue burning
CRM	crop residue management
CTM	chemical transport model
EI	emission inventory
EOS	earth observation satellites
ESRI	Environment Systems Research Institute
FAR	false alarm ratio
FINN	Fire INventory from the NCAR
FN	false negative
FNR	false negative rate
FP	false positive
FPOs	farmer producer organisations
FPR	false positive rate
FRP	fire radiative power
GEE	Google Earth Engine
GEO-KOMPSAT-2A	Geostationary Korea Multi-Purpose Satellite-2A
GHG	greenhouse gas
GRAP	*Graded Response Action Plan*
HLS	Harmonised Landsat and Sentinel-2
IGP	Indo-Gangetic Plain
IITM	Indian Institute of Tropical Meteorology
IMD	Indian Meteorological Department
ISRO	Indian Space Research Organisation
LULC	land use–land cover
MIRBI	Mid-Infrared Burn Index
MoAFW	Ministry of Agriculture and Family Welfare
MODIS	Moderate Resolution Imaging Spectroradiometer
MoPNG	Ministry of Petroleum and Natural Gas
NBR	Normalised Burn Ratio
NBR2	Normalised Burn Ratio 2
NCAR	National Centre for Atmospheric Research
NGT	National Green Tribunal
NRSC	National Remote Sensing Centre
PM	particulate matter
POD	probability of detection
ROC	receiver operating characteristic
ROI	region of interest
SATAT	*Sustainable Alternative Towards Affordable Transportation*
SMAM	*Sub-Mission on Agricultural Mechanization*
SUOMI NPP	Suomi National Polar-Orbiting Partnership
T1	threshold 1
T2	threshold 2
T3	threshold 3
T4	threshold 4
T5	threshold 5
T6	threshold 6
TBI	Tasselled Cap Brightness Index
TN	true negative
TP	true positive
TPP	thermal power plant
TPR	true positive rate
VIIRS	Visible Infrared Imaging Radiometer Suite

References

Abdurrahman, Muhammad Isa, Sukalpaa Chaki, and Gaurav Saini. 2020. “Stubble Burning: Effects on Health & Environment, Regulations and Management Practices.” *Environmental Advances* 2 (December): 100011. https://doi.org/10.1016/j.envadv.2020.100011.

Alcaras, Emanuele, Domenica Costantino, Francesca Guastaferro, Claudio Parente, and Massimiliano Pepe. 2022. “Normalized Burn Ratio Plus (NBR+): A New Index for Sentinel-2 Imagery.” *Remote Sensing* 14 (7): 7. https://doi.org/10.3390/rs14071727.

Ali, Basma A., Mohamed Hosny, Hussein N. Nassar, Heba K. A. Elhakim, and Nour Sh. El-Gendy. 2024. “A Study on the Valorization of Rice Straw into Different Value-Added Products and Biofuels.” *International Journal of Chemical Engineering* 2024 (1): 9185870. https://onlinelibrary.wiley.com/doi/10.1155/2024/9185870.

Ambulkar, Rupal, Gaurav Govardhan, Srujan Gavhale, et al. 2025. “Crop Residue Burning in North-Western India: Emission Estimation and Uncertainty Quantification.” *Journal of Geophysical Research: Atmospheres* 130 (4): e2024JD042198. https://doi.org/10.1029/2024JD042198.

Andini, Ade, Sebastien Bonnet, Patrick Rousset, and Udin Hasanudin. 2018. “Impact of Open Burning of Crop Residues on Air Pollution and Climate Change in Indonesia.” *Current Science* 115 (12): 2259–2266. https://doi.org/10.18520/cs/v115/i12/2259-2266.

CAQM. 2021a. “Standard Protocol for Estimation of Crop Residue Burning Fire Events using Satellite Data”.Commission for Air Quality Management in NCR and Adjoining Areas, August 16. https://caqm.nic.in/WriteReadData/LINKS/35a41e6ccf-e4cf-47ad-8ad0-4acc6a1625b0.pdf.

CAQM. 2021b. “Press Release.” Commission for Air Quality Management. November 3. https://caqm.nic.in/WriteReadData/LINKS/20ba71d805-a767-4bb1-921e-5d49558fdf8e.pdf.

CAQM. 2022. “Press Release.” Commission for Air Quality Management. March 22. https://caqm.nic.in/WriteReadData/LINKS/8%20CAQM%20PR%2022%20Mar%20(1)3ed5f1a2-18b1-414d-85ae-3abae541df05.pdf.

CAQM. 2025. Direction under Section 12 of Commission for Air Quality Management in NCR and Adjoining Areas Act, 2021 - Implementation of the plan of action for prevention and control of Paddy Stubble Burning in 2025, targeting complete elimination - reg. May 9. https://caqm.nic.in/WriteReadData/LINKS/Direction%20No-904d88bdb5-5814-4f30-b05d-49917ac33c03.pdf.

CCAC. 2023. “Indian Agricultural Residue Potential to Supplement Energy Sector.” Climate and Clean Air Coalition, August 29. https://www.ccacoalition.org/news/indian-agricultural-residue-potential-supplement-energy-sector.

Chen, Yang, Stijn Hantson, Niels Andela, et al. 2022. “California Wildfire Spread Derived Using VIIRS Satellite Observations and an Object-based Tracking System.” *Scientific Data* 9 (May): 249. https://doi.org/10.1038/s41597-022-01343-0.

Copernicus. n.d. “EFFIS – Active Fire Detection.” Accessed August 25 2025. https://forest-fire.emergency.copernicus.eu/about-effis/technical-background/active-fire-detection.

CREAMS. n.d. “Home.” Consortium for Research on Agroecosystem Monitoring and Modeling from Space. Accessed 15 July 2025. https://creams.iari.res.in/.

Deshpande, Monish Vijay, Dhanyalekshmi Pillai, and Meha Jain. 2022. “Agricultural Burned Area Detection Using an Integrated Approach Utilizing Multi Spectral Instrument Based Fire and Vegetation Indices from Sentinel-2 Satellite.” MethodsX 9 (January): 101741. https://doi.org/10.1016/j.mex.2022.101741.

Dhaliwal, H. S. n.d. *The Happy Seeder and Its Benefits: Results from the Demonstration Project In Punjab*. Climate and Clean Air Coalition.

Erbaugh, James, Gurpreet Singh, Zhixian Luo, Gurulingappa Koppa, Jeffrey Evans, and Priya Shyamsundar. 2024. “Farmer Perspectives on Crop Residue Burning and Sociotechnical Transition in Punjab, India.” *Journal of Rural Studies* 111 (October): 103387. https://doi.org/10.1016/j.jrurstud.2024.103387.

ESA. n.d. “Sentinel-2.” European Space Agency. Accessed 14 July 2025. https://www.esa.int/Applications/Observing_the_Earth/Copernicus/Sentinel-2.

Fusco, Emily J., John T. Finn, John T. Abatzoglou, Jennifer K. Balch, Sepideh Dadashi, and Bethany A. Bradley. 2019. “Detection Rates and Biases of Fire Observations from MODIS and Agency Reports in the Conterminous United States.” *Remote Sensing of Environment* 220 (January): 30–40. https://doi.org/10.1016/j.rse.2018.10.028.

Govardhan, Gaurav, Rupal Ambulkar, Santosh Kulkarni, et al. 2023. “Stubble-burning Activities in North-western India in 2021: Contribution to Air Pollution in Delhi.” *Heliyon* 9 (6). https://doi.org/10.1016/j.heliyon.2023.e16939.

Govardhan, Gaurav, Sachin D. Ghude, Rajesh Kumar, et al. 2024. "Decision Support System Version 1.0 (DSS v1.0) for Air Quality Management in Delhi, India." *Geoscientific Model Development* 17 (7): 2617–2640. https://doi.org/10.5194/gmd-17-2617-2024.

Gupta, Ridhima. 2010. "The Economic Causes of Crop Residue Burning in Western Indo-Gangetic Plains." Presented at the 5th Annual Conference on Economic Growth and Development, Indian Statistical Institute, Delhi Centre, 15–17 December 2010.

GWIS. n.d. "GWIS – Active Fire Detection." Global Wildfire Information System. Accessed 16 July 2025. https://gwis.jrc.ec.europa.eu/about-gwis/technical-background/active-fire-detection.

Hindustan Times. 2023. "Over 4k Nodal Officers to Help Punjab Check Stubble Burning." *Hindustan Times*, September 9. https://www.hindustantimes.com/cities/chandigarh-news/over-4k-nodal-officers-to-help-punjab-check-stubble-burning-101694199692497.html.

Hua, Wenxuan, Sijia Lou, Xin Huang, et al. 2024. "Diagnosing Uncertainties in Global Biomass Burning Emission Inventories and Their Impact on Modeled Air Pollutants." *Atmospheric Chemistry and Physics* 24 (11): 6787–6807. https://doi.org/10.5194/acp-24-6787-2024.

ICAR. 2021. *Ex-Situ Crop Residue Management Options*. Indian Council of Agricultural Research.

ICAR. 2024. *Monitoring Paddy Residue Burning in India Using Satellite Remote Sensing During 2024*. Indian Council of Agricultural Research.

Jaffe, Daniel A., Susan M. O'Neill, Narasimhan K. Larkin, et al. 2020. "Wildfire and Prescribed Burning Impacts on Air Quality in the United States." *Journal of the Air & Waste Management Association* 70 (6): 583–615. https://doi.org/10.1080/10962247.2020.1749731.

Jethva, Hiren, Omar Torres, Robert D. Field, Alexei Lyapustin, Ritesh Gautam, and Vinay Kayetha. 2019. "Connecting Crop Productivity, Residue Fires, and Air Quality over Northern India | *Scientific Reports*." Scientific Reports 9. https://www.nature.com/articles/s41598-019-52799-x.

Kemanth, Kurinji, Ramandeep Singh, and Sneha Maria Ignatious. 2024. *How Can Punjab End Stubble Burning with Crop Residue Management*? Council on Energy, Environment and Water.

Kingra, P. K., Raj Setia, Simranjeet Singh, et al. 2017. "Climatic Variability and its Characterisation over Punjab, India." *Journal of Agrometeorology* 19 (3): 3. https://doi.org/10.54386/jam.v19i3.664.

Kouadio, Bob Kouakou, Sié Ouattara, Alain Clément, Jean-Marc Gala Bi Zaouri, Jean-Luc Kouadio Kouassi Jean-Luc, and Edouard Kouakou N'guessan. 2023. "Detection of Burned Areas through Spectral Indices Analysis of Sentinel-2A Satellite Images in the Abokouamékro Wildlife Reserve (Central, Côte d'Ivoire)." *Open Journal of Applied Sciences* 14 (1): 1. https://doi.org/10.4236/ojapps.2024.141016.

Kumar, Parmod, Surender Kumar, and Laxmi Joshi. 2015. "The Extent and Management of Crop Stubble." *In Socioeconomic and Environmental Implications of Agricultural Residue Burning: A Case Study of Punjab, India*, edited by Parmod Kumar, Surender Kumar, and Laxmi Joshi. Springer India. https://doi.org/10.1007/978-81-322-2014-5_2.

Kumar, Sumit, Sanjay Kumar Ghosh, and Brijendra Pateriya. 2025. "Development of New Spectral Indices for Mapping of Crop Residue Burning Using Satellite Remote Sensing." *International Journal of Remote Sensing* 46 (10): 3851–3873. https://doi.org/10.1080/01431161.2025.2492411.

Kurinji, L. S., and Srish Prakash. 2021. *Why Paddy Stubble Continues to Be Burnt in Punjab*? Council on Energy, Environment and Water.

Li, Rong, Xinjie He, Hong Wang, et al. 2022. "Estimating Emissions from Crop Residue Open Burning in Central China from 2012 to 2020 Using Statistical Models Combined with Satellite Observations." *Remote Sensing* 14 (15): 15. https://doi.org/10.3390/rs14153682.

Lin, Muyang, and Toritseju Begho. 2022. "Crop Residue Burning in South Asia: A Review of the Scale, Effect, and Solutions with a Focus on Reducing Reactive Nitrogen Losses." *Journal of Environmental Management* 314 (July): 115104. https://doi.org/10.1016/j.jenvman.2022.115104.

Liu, Tianjia, Miriam E Marlier, Alexandra Karambelas, et al. 2019. "Missing Emissions from Post-Monsoon Agricultural Fires in Northwestern India: Regional Limitations of MODIS Burned Area and Active Fire Products." *Environmental Research Communications* 1 (1): 011007. https://doi.org/10.1088/2515-7620/ab056c.

Liu, Tianjia, Loretta J. Mickley, Sukhwinder Singh, Meha Jain, Ruth S. DeFries, and Miriam E. Marlier. 2020. "Crop Residue Burning Practices across North India Inferred from Household Survey Data: Bridging Gaps in Satellite Observations." *Atmospheric Environment*: X 8 (December): 100091. https://doi.org/10.1016/j.aeaoa.2020.100091.

Luft, Harrison, Calogero Schillaci, Guido Ceccherini, Diana Vieira, and Aldo Lipani. 2022. "Deep Learning Based Burnt Area Mapping Using Sentinel 1 for the Santa Cruz Mountains Lightning Complex (CZU) and Creek Fires 2020." *Fire* 5 (5): 163. https://doi.org/10.3390/fire5050163.

Misra, Prakhar, Sachiko Hayashida, Masao Moriyama, and Hikaru Araki. 2025. "Limitations of Interpreting Orbiting Satellite-Based Fire Detection for Crop Residue Burning: Has Agricultural Burning in North-west India Decreased in Recent Years?" *SSRN Scholarly Paper*: 5114136. https://doi.org/10.2139/ssrn.5114136.

MNRE. n.d. "Sardar Swaran Singh National Institute of Bio-Energy." Ministry of New and Renewable Energy. Accessed 17 July 2025. https://nibe.res.in/english/biomass-atlas.php.

MoAFW. 2018. "Sub-Mission on Agricultural Mechanization." Ministry of Agriculture and Farmers Welfare.

Mohammad, Lal, Jatisankar Bandyopadhyay, Rubel Sk, et al. 2023. "Estimation of Agricultural Burned Affected Area Using NDVI and dNBR Satellite-Based Empirical Models." *Journal of Environmental Management* 343 (October): 118226. https://doi.org/10.1016/j.jenvman.2023.118226.

MoPNG. n.d. "Refining – Compressed Bio Gas." Ministry of Petroleum & Natural Gas. Accessed 10 July 2025. https://mopng.gov.in/en/refining/compressed-bio-gas/1000.

MoPNG. 2018. "National Policy on Biofuels – 2018." Ministry of Petroleum & Natural Gas. April 6.https://mopng.gov.in/files/uploads/NATIONAL_POLICY_ON_BIOFUELS-2018.pdf.

MoPNG. 2024. "Scheme Guidelines for Providing Financial Assistance to Compressed Bio Gas (CBG) Producers for Procurement of Biomass Aggregation Machinery [press release]." Ministry of Petroleum & Natural Gas. February 2.https://satat.co.in/satat/assets/download/Scheme%20guidelines.pdf.

NASA. n.d. "Documents – Harmonized Landsat Sentinel-2." National Aeronautics and Space Administration. Accessed 28 August 2025. https://hls.gsfc.nasa.gov/documents/.

NASA. n.d.a. "NASA-FIRMS." National Aeronautics and Space Administration. Accessed 9 July 2025. https://firms.modaps.eosdis.nasa.gov/map/.

NASA. n.d.b. "Sentinel-2 MSI NASA Earthdata." National Aeronautics and Space Administration. Accessed 7 July 2025. https://www.earthdata.nasa.gov/data/instruments/sentinel-2-msi.

NASA. 2024. "Is Fire Activity Declining in Northwestern India?" *Earth Observatory*, November 8. https://earthobservatory.nasa.gov/images/153826/is-fire-activity-declining-in-northwestern-india.

NASA Earthdata. 2022. "Characteristics of VIIRS, MODIS, and OLI Sensors and Their Effects on the Spatial Extent of Daily Active Fire Data." *Earthdata*, September 29. https://www.earthdata.nasa.gov/news/blog/characteristics-viirs-modis-oli-sensors-effects-spatial-extent-daily-active-fire-data.

NASA Earthdata. 2024. "VIIRS I-Band 375 m Active Fire Data." *Earthdata*, October 21. https://www.earthdata.nasa.gov/data/instruments/viirs/viirs-i-band-375-m-active-fire-data.

Newslaundry. 2022. "Punjab's Farmers Are Burning Less Stubble. Thanks to Super Seeders." *Newslaundry*, November 14. https://www.newslaundry.com/2022/11/14/punjabs-farmers-are-only-partially-burning-stubble-thanks-to-super-seeders.

NGT. 2023. "News Item Published in The Hindu dated 06.10.2023 titled "Pollution takes a front seat as Stubble Fires Spike in Punjab"." National Green Tribunal, October 18. https://www.greentribunal.gov.in/sites/default/files/news_updates/Report%20by%20PPCB%20in%20OA%20No.%20632%20of%202023%20(In%20re%20News%20Item%20published%20in%20The%20Hindu%20dated%2006.10.2023%20titled%20Pollution%20takes%20a%20front%20seat%20as%20Stubble%20Fires%20Spike%20in%20Punjab).pdf.

NGT. 2024. "News Item Published in The Hindu dated 06.10.2023 titled "Pollution takes a front seat as Stubble Fires Spike in Punjab"." National Green Tribunal, March 19. https://www.greentribunal.gov.in/sites/default/files/news_updates/Action%20Taken%20Report%20on%20behalf%20of%20Punjab%20Pollution%20Control%20Board%20in%20OA%20No.%20632%20of%202023%20(In%20re%20%20News%20item%20appearing%20in%20Hindu%20dated%2006.10.2023%20....pdf.

NRSC-ISRO. 2022. "Assessment of Paddy Stubble Burnt Area Progression in Punjab – Kharif 2022 Agricultural Sciences & Applications Group, Remote Sensing Applications Area." National Remote Sensing Centre–Indian Space Research Organisation.

Parkinson, Claire L. 2022. "The Earth-Observing Aqua Satellite Mission: 20 Years and Counting." *Earth and Space Science* 9 (9): e2022EA002481. https://doi.org/10.1029/2022EA002481.

Payra, Swagata, Ajay Sharma, Manoj Kumar Mishra, and Sunita Verma. 2023. "Performance Evaluation of MODIS and VIIRS Satellite AOD Products over the Indian Subcontinent." *Frontiers in Environmental Science* 11 (June). https://doi.org/10.3389/fenvs.2023.1158641.

Pinakana, Sai Deepak, Amit U. Raysoni, Alqamah Sayeed, et al. 2024. "Review of Agricultural Biomass Burning and Its Impact on Air Quality in the Continental United States of America." *Environmental Advances* 16 (July): 100546. https://doi.org/10.1016/j.envadv.2024.100546.

Pinto, Miguel M., Ricardo M. Trigo, Isabel F. Trigo, and Carlos C. DaCamara. 2021. "A Practical Method for High-resolution Burned Area Monitoring Using Sentinel-2 and VIIRS." Remote Sensing 13 (9): 1608. https://www.mdpi.com/2072-4292/13/9/1608.

PIB. 2019. “Ban on Crop Residue Burning [press release].” *Press Information Bureau*, June 21. https://www.pib.gov.in/newsite/PrintRelease.aspx?relid=190615.

PIB. 2021. “Agricultural Mechanization for In-Situ Management of Crop Residue [press release].” *Press Information Bureau*, March 23. https://www.pib.gov.in/Pressreleaseshare.aspx?PRID=1707021.

PIB. 2023a. “CAQM Announces Revision of the Graded Response Action Plan (GRAP) to Further Strengthen Measures to Combat Sudden/ Anticipated Deterioration of Air Quality in NCR during Winter Months [press release].” *Press Information Bureau*, July 28. https://www.pib.gov.in/www.pib.gov.in/Pressreleaseshare.aspx?PRID=1943721.

PIB. 2023b. “Punjab Submits State Action Plan and District-Wise Action Plans for Tackling the Problem of Stubble Burning to the Commission (CAQM) for the Current Paddy Harvesting Season [press release].” *Press Information Bureau*, September 26. https://www.pib.gov.in/www.pib.gov.in/Pressreleaseshare.aspx?PRID=1960891.

PIB. 2024. “Parliament Question: Air Pollution Caused by Stubble Burning [press release].” *Press Information Bureau*, November 25. https://www.pib.gov.in/www.pib.gov.in/Pressreleaseshare.aspx?PRID=2076918.

PIB. 2025. “Stubble Burning [press release].” *Press Information Bureau*, March 18. https://www.pib.gov.in/www.pib.gov.in/Pressreleaseshare.aspx?PRID=2112397.

Schroeder, Wilfrid, Patricia Oliva, Louis Giglio, and Ivan A. Csiszar. 2014. “The New VIIRS 375 m Active Fire Detection Data Product: Algorithm Description and Initial Assessment.” *Remote Sensing of Environment* 143 (March): 85–96. https://doi.org/10.1016/j.rse.2013.12.008.

SCO. 2024. “Delhi Pollution Crisis: Can the Supreme Court Clear the Air?” *Supreme Court Observer*, November 23. https://www.scobserver.in/journal/delhi-pollution-crisis-can-the-supreme-court-clear-the-air/.

Sehgal, Vinay Kumar, Rajkumar Dhakar, Aakash Chhabbra, Niveta Jain, Rabi Narayan Sahoo, and Joydeep Mukherjee. 2021. “Geospatial Approach for Monitoring of Crop Residue Burning for Its Management Including Conservation Agriculture.” *Journal of Agricultural Physics* 21 (1): 274–284.

Singh, Dharmendra, Nidhi Kundu, and Santanu Ghosh. 2021. “Mapping Rice Residues Burning and Generated Pollutants Using Sentinel-2 Data over Northern Part of India.” *Remote Sensing Applications: Society and Environment* 22 (April): 100486. https://doi.org/10.1016/j.rsase.2021.100486.

Singh, Gurraj, Manish Kumar Gupta, Santan Chaurasiya, Vishal S Sharma, and Danil Pimenov. 2021. “Rice Straw Burning: A Review on Its Global Prevalence and the Sustainable Alternatives for Its Effective Mitigation.” *Environmental Science and Pollution Research* 28: 32125–32155. https://link.springer.com/article/10.1007/s11356-021-14163-3.

Singh, Manpreet, A. T. Chaleka, Rajesh Goyal, et al. 2024. “PAU Smart Seeder: A Novel Way Forward for Rice Residue Management in North-West India.” *Nature Scientific Reports*. https://www.nature.com/articles/s41598-024-62337-z.

TERI. 2021. *Does Air Quality from Crop Residue Burning in Close Proximity to Residential Areas Adversely Affect Respiratory Health*? The Energy and Resources Institute.

UPAg, DoAFW. n.d. “All India APY.” Unified Portal for Agricultural Statistics, Department of Agriculture and Farmers Welfare. Accessed 16 July 2025. https://dash.upag.gov.in/statewiseapyandpercentagetoallindia?t=&stateID=0&.

USDA. 2025. “Rice – Rice Sector at a Glance.” United States Department of Agriculture. https://www.ers.usda.gov/topics/crops/rice/rice-sector-at-a-glance.

Wiedinmyer, Christine, Yosuke Kimura, Elena C. McDonald-Buller, et al. 2023. “The Fire Inventory from NCAR Version 2.5: An Updated Global Fire Emissions Model for Climate and Chemistry Applications.” *Geoscientific Model Development* 16 (13): 3873–3891. https://doi.org/10.5194/gmd-16-3873-2023.

World Bank. n.d. “Agricultural Pollution Field Burning.” Accessed July 14 2025. https://documents1.worldbank.org/curated/en/989351521207797690/pdf/124342-repl-WB-Knowledge-Burning.pdf.

Zhang, Ning, Lin Sun, Zhendong Sun, and Yu Qu. 2021. “Detecting Low-intensity Fires in East Asia Using VIIRS Data: An Improved Contextual Algorithm.” *Remote Sensing* 13 (21): 4226. https://doi.org/10.3390/rs13214226.

Image: iStock

The authors

Sneha Maria Ignatious

sneha.ignatious@ceew.in

Sneha Maria Ignatious

Sneha is a Programme Associate with CEEW's Clean Air Team. She uses data-driven approaches to draw insights and generate evidence to drive policies on air quality management. Sneha holds a master's degree in green energy technology from Pondicherry University and a bachelor's degree in electronics and communication engineering.

Rishikesh P.

rishikesh.p@ceew.in

Rishikesh P.

Rishikesh P. is a Research Analyst with CEEW's Clean Air team. His work focuses on providing science-based evidence using air quality modelling (chemical transport models) and remote sensing techniques for air quality-related studies. He holds a master's degree in environmental engineering from the Indian Institute of Technology (IIT), Madras, and a bachelor's degree in civil engineering from the National Institute of Technology (NIT), Calicut.

Mohammad Rafiuddin

mohammad.rafiuddin@ceew.in

Rafiuddin Mohammad

Mohammad Rafiuddin is a Programme Lead with CEEW's Clean Air team. His work focuses on designing data-driven solutions to improve air quality in Indian cities. He has a PhD in atmospheric sciences from the Jawaharlal Nehru Centre for Advanced Scientific Research (JNCASR), Bengaluru, and a bachelor's degree in mechanical engineering from the Jawaharlal Nehru Technological University (JNTU), Hyderabad.

COUNCIL ON ENERGY, ENVIRONMENT AND WATER (CEEW)

ISID Campus, 4 Vasant Kunj Institutional Area
New Delhi - 110070, India
T: +91 (0) 11 4073 3300

info@ceew.in | ceew.in | @CEEWIndia | ceewindia

Scan to download the study